https://doi.org/10.1016/j.trc.2022.104011

Departure Time Choices in the Morning Commute with a Mixed Distribution of Capacity

Qiumin Liu[a], Rui Jiang[a,*], Wei Liu[b], Ziyou Gao[a]

[a] *Key Laboratory of Transport Industry of Big Data Application Technologies for Comprehensive Transport, Ministry of Transport, Beijing Jiaotong University, Beijing 100044, China*

[b] *Department of Aeronautical and Aviation Engineering, The Hong Kong Polytechnic University, Hong Kong, China*

Abstract

Incidents and other random factors may create variations to the transportation system and thus result in stochastic road capacity during the travel period. The realized capacity on a given day (i.e., an average value over the travel period) changes from day to day. For instance, existing empirical studies indicate that incident capacity reduction can be approximated as a continuous random variable. This study examines the morning commute problem with a road bottleneck whose capacity is constant within a day but changes stochastically from day to day. This study extends existing stochastic bottleneck model studies by considering a more general distribution of the bottleneck capacity. In particular, the capacity of bottleneck is at the designed value under good external conditions and degrades into a smaller value within an interval (i.e., the capacity degradation range) under adverse external conditions (a "mixed" distribution). Commuters' departure time choices follow the Wardrop's first principle in terms of their mean individual travel cost. Given the considered distribution of capacity, additional equilibrium departure/arrival patterns against the literature have been identified and examined. How the mean travel cost and the mean of total travel time may vary with the capacity degradation probability and the level of capacity degradation have been analyzed. The impacts of the width of degraded capacity range have also been investigated to quantify how the results are affected if the degraded capacity is assumed as the mean value (rather than a degraded capacity range). Our results indicate that with less severe capacity degradation, the mean travel cost always decreases and improving the capacity under "worst conditions" can be more effective than improving the capacity under the "best adverse condition". However, it is not always the case for reducing the total travel time, and the mentioned measures may exacerbate the system's congestion, especially when the capacity degradation rarely occurs. Under a given mean capacity, the mean travel cost would be underestimated if the capacity degradation range is ignored. We also compare system performance considering different capacity distributions. It is found that the "mixed" capacity distribution defined in this study outperforms the binary capacity distribution in terms of evaluating the departure/arrival pattern and the mean travel cost. This study enhances our understanding on the morning commute problem under capacity uncertainty.

Keywords: Stochastic bottleneck model; Capacity distribution; Mean travel cost; User Equilibrium

1. Introduction

Traffic congestion has been increasingly severe in urban areas, which escalates commuting cost of travelers. The bottleneck model was firstly developed by Vickrey (1969) to capture commuters' departure

* Corresponding author.
Email address: jiangrui@bjtu.edu.cn

time choices and quantify the congestion dynamics during the morning peak hours. In the bottleneck model, commuters travel from home to workplace every day through a highway bottleneck with a fixed capacity. Congestion is modelled in the form of point queue when the departure rate exceeds the capacity of bottleneck. At equilibrium, all commuters experience the same travel cost that consists of queuing delay cost and schedule delay cost. Vickrey's bottleneck model provides a tractable way to obtain analytical insights and policy implications regarding travel choices, supply and demand planning/management. Many studies have taken advantage of the bottleneck model's tractability to generate understanding on various aspects of commuting problems, including travel behavior analysis, demand-side management strategies, supply-side management strategies, and joint management strategies of demand and supply sides. One may refer to Li et al. (2020) for a more comprehensive review of bottleneck studies.

There is a branch of studies concerning the impacts of uncertainty (due to demand variations, traffic accidents, adverse weather conditions, road maintenance, etc.) on user choices and performance of the transportation system in the context of the bottleneck model.[1] For instance, Lindsey (1994) investigated the user equilibrium and social optimum departure/arrival patterns when the highway bottleneck capacity follows a binary distribution (high and low capacities). Arnott et al. (1999) and Fosgerau (2008; 2010) extended the classic bottleneck model by considering both supply and demand uncertainties. In order to examine the impact of uncertainty on travel decisions and departure/arrival patterns, Sui and Lo (2009) examined the case where commuters experience exogenous random travel delay that is constant within a day. This idea was further extended by Jiang et al. (2016), where the random delay is queue-dependent and the variability of travel cost is incorporated. And commuters' departure time choice is governed by both the expected travel cost and the variability of travel cost. Peer et al. (2010) examined traffic patterns in the bottleneck model with time-varying stochastic capacity given that traffic incident leading to capacity drop is stochastic.

When modeling commuters' travel behaviors in a bottleneck model with stochastic capacity, different behavioral assumptions have been adopted in the literature. It is often assumed that commuters are risk neutral and minimize their mean travel cost (Xiao et al., 2014a, 2014b, 2015; Zhu et al., 2019; Long et al., 2022). In order to capture commuters' risk attitudes towards stochasticity, Li et al. (2008, 2017) and Ma et al. (2021) examined the case where commuters choose their departure times by minimizing a combination of the expected travel cost and the standard deviation of travel time. Based on the experimental findings, Liu et al. (2020) analyzed equilibrium departure/arrival patterns where commuters make their departure time choices based on the travel cost budget, which is defined as a weighted average of the mean and standard deviation of the travel cost. Recently, in order to capture the variations in both queuing cost and scheduling cost endogenously under an uncertain road capacity, Jiang et al., (2022) defined the value of capacity reliability and proposed the generalized cost as a linear combination of mean travel cost and variation cost. In their model, the variation cost is defined as the difference between the maximum and minimum travel costs and commuters are assumed to make departure time choice by minimizing the generalized cost. The current study follows the majority of existing stochastic bottleneck model studies and considers risk neutral commuters who minimize their mean travel cost (the long term mean over calendar time).

This study extends the literature by considering a refined highway bottleneck capacity distribution. In

[1] Many studies have been carried out to investigate the impact of traffic uncertainty, which are not limited to the bottleneck model setting. Lo and Tung (2003) analyzed probabilistic user equilibrium (PUE) in transportation network with degradable links in which travelers make the route choice based on the mean travel time in face of uncertain travel time. This work was extended by Lo et al. (2006), in which the concept of travel time budget (TTB) that relates the travel time variability with travelers' route choice behaviors was proposed. In a similar way, several other risk-taking route choice criteria have been proposed to assess transportation network performance under uncertainty, such as mean-excess travel time model (Chen et al., 2010, 2011); percentile travel time model (Nie, 2011); expected utility theory (Yin et al., 2004; Watling, 2006).

existing stochastic bottleneck models, a binary distribution of capacity has been studied by Lindsey (1994), a uniform distribution of capacity is examined by Xiao et al. (2015), and a general continuous distribution of capacity is considered by Long et al. (2022). In these three studies, the capacity is assumed to follow either a discrete distribution or continuous distribution. We argue that adverse conditions/factors that cause road capacity degradation do not arise every day. When such factors do not arise, the road capacity is equal to the designed capacity. When such factors do arise on a particular day, they may differ in terms of the level of seriousness as well as the negative impacts on the road capacity, i.e., the road capacity drops to different extents and is subject to a certain distribution that can be approximated as continuous. In particular, incidents are one of the main causes of uncertainty in the transportation system and can result in the stochastic capacity in the travel period. The realized (average) capacity during the travel period on a given day may change from day to day. Based on the data collected in Hampton Roads region of Virginia, Qin and Smith (2001) estimated the capacity reductions caused by accidents and disabled vehicles when one-lane and two-lane out of three lanes have been blocked. Their study showed that the observed reductions in capacity can be best represented by continuous random variables, and the Beta distribution provides a good fit of accident capacity reductions due to one or two lanes (out of three lanes) being blocked. When one lane (out of three lanes) is blocked, the minimum observed reduction in capacity is 28.76%, which indicates that there exists a capacity gap between the designed capacity and the accident capacity, while the accident capacity can be approximated as a continuous random variable.

This paper considers a "mixed" bottleneck capacity distribution and examines the resulting commuting patterns. In particular, we consider a "mixed" capacity distribution, under which the road capacity is at the designed value with a certain probability (e.g., good traffic conditions without accidents), and degrades into a smaller value otherwise (e.g., adverse traffic conditions when accidents occur), where this value falls into an interval (capacity degradation range) and follows a continuous distribution. Under such a capacity setting, we consider that commuters choose their departure times to minimize the mean travel cost, and then derive and analyze the possible equilibrium departure/arrival patterns. The impacts of the width of degraded capacity range, the capacity degradation probability and the ratios of capacity degradation on the mean travel cost and on the total queuing time are also investigated. Moreover, in the numerical studies, by taking advantage of the empirical findings in Qin and Smith (2001), we compare the system performance (e.g., costs, departure/arrival patterns) under different capacity distributions (the one obtained from the observed capacity distribution, the "mixed" distribution considered in this paper, and that obtained when the degraded capacity range is ignored, i.e., the capacity after degradation is fixed). Note that the departure/arrival pattern and mean travel cost are based on the proposed model in this paper, while the capacity distribution is based on the accident capacity data in Qin and Smith (2001). It is found that the mean travel cost is always underestimated if the degraded capacity range is ignored and an average capacity is assumed. The proposed "mixed" capacity distribution better reproduces the departure/arrival pattern and mean travel cost than those obtained when the degraded capacity range is not considered. It is also observed that the cumulative departures at each departure time and the mean travel cost under different probabilities of incidents is always overestimated by the "mixed" capacity distribution when compared to those under the "true" observed capacity data.

The rest of this paper is organized as follows. In Section 2, the stochastic bottleneck model with a "mixed" distribution of bottleneck capacity is analyzed. All possible equilibrium departure/arrival patterns and their corresponding parameter ranges are discussed in detail. Section 3 investigates the impacts of the capacity degradation probability, the ratios of degraded capacity, and the width of the degraded capacity range on the mean travel cost and on the mean of total travel time. Numerical examples are given in Section

4 to further illustrate the analysis, and the comparisons of the results under different capacity distributions are also illustrated by using the empirical data in the literature. Finally, Section 5 concludes.

2. Stochastic bottleneck model with "mixed" distribution of capacity

2.1 Bottleneck models with stochastic capacity

We first list the major notations used in this paper.

Notational glossary

α	The value of travel time	t_e	Departure time of the latest commuter
β	The value of schedule delay early	t_j^i	The j-th critical time point defined for departure/arrival Pattern i.
γ	The value of schedule delay late	$\hat{s}$	The smallest capacity at which the latest commuter departing at t_e could just avoid queuing
$\bar{s}$	The designed capacity	Θ	$\Theta = \frac{1}{\theta_2-\theta_1} ln \frac{\theta_2}{\theta_1}$
θ_1	The ratio of the worst degraded capacity to the designed capacity	π_C	$\pi_C = \frac{\gamma}{\alpha+\gamma}$
θ_2	The ratio of the best degraded capacity to the designed capacity	π_S	$\pi_S = \frac{\beta}{(\alpha+\gamma)(\Theta-1)}$
π	The probability of capacity degradation	π_R	$\pi_R = \frac{\beta}{(\alpha+\gamma)(\theta_2\Theta-1)}$
$r_i(t)$	Departure rate in situation i at time t	π_M	$\pi_M = \frac{\beta}{(\alpha-\beta)(\theta_2\Theta-1)}$
$r_i^j(t)$	Departure rate in situation i-j at time t	π_N	$\pi_N = \frac{\beta}{(\alpha-\beta)(\Theta-1)}$
$R(t)$	Cumulative departure at time t	π_T	$\pi_T = \frac{\gamma(\theta_2-\theta_1)}{\theta_1(\alpha+\gamma)\chi}$, where χ solves the equation $(1+1/\chi)\, ln(1+\chi) = (\beta+\gamma)/\gamma$
t^*	Official work start time	π_L	$\pi_L = \frac{\beta}{(\alpha+\gamma)\Theta-(\alpha-\beta)-(\beta+\gamma)/\theta_2}$
t_s	Departure time of the first commuter	e	$e=\frac{\theta_2+\theta_1}{2}$
$T(t)$	Queuing time at t and $T(t) = R(t)/s - (t - t_s)$	m	$m=\theta_2 - \theta_1$
$\hat{t}$	$\hat{t} = t^* - t_s$	φ	$\varphi = \pi(\alpha+\gamma)(\Theta-1)$

We now summarize the major assumptions in this paper.

Assumption A1: Commuters are homogeneous in terms of value of time, values of early and late arrival schedule delays.

Assumption A2: Commuters are assumed to be risk neutral, and they consider the long-term mean travel cost when making departure time choices (note that the mean is subject to the capacity distribution). Thus,

commuters' departure time choice follows the Wardrop's first principle in terms of the mean travel cost.

Assumption A3: The capacity of bottleneck is constant within a day but changes stochastically from day to day. We assume that the capacity follows a "mixed" distribution, which is at the designed capacity $\bar{s}$ under good conditions with probability $1-\pi$, and degrades into an interval $(\theta_1\bar{s}, \theta_2\bar{s})$ under adverse conditions with probability π, where $0 \le \pi \le 1$ and $0 < \theta_1 \le \theta_2 < 1$. For simplicity, we assume that the capacity follows the uniform distribution within $(\theta_1\bar{s}, \theta_2\bar{s})$ under adverse conditions, which can be generalized to other continuous distributions as in Long et al. (2022). The distribution of stochastic capacity in this paper reduces to that in Xiao et al. (2015) if $\pi = 1$ and $\theta_2 = 1$ and reduces to that in Lindsey (1994) if $\theta_1 = \theta_2$.

Based on the above assumptions, the equilibrium condition for commuters' departure time choice in a single bottleneck with stochastic capacity can be given as follows: no commuter can reduce his/her mean travel cost (long-term mean over calendar time) by unilaterally altering his or her departure time at equilibrium. This condition implies that commuters' mean travel cost is constant with respect to the time instant if the departure rate is positive, i.e., $dE(C(t))/dt = 0$ if $r(t) > 0$, where $E(C(t))$ and $r(t)$ denote the expected travel cost and the departure rate for commuters departing at time *t*, respectively.

As the capacity of bottleneck is constant within a day, but fluctuates from day to day, commuters departing at the same time may encounter schedule delay early or late and may or may not encounter queuing delay on different days. The possible combinations of schedule delay and queuing experiences (for commuters) in the stochastic bottleneck are summarized in Table 1. Three types of schedule delay and two types of queuing experience could lead to six combinations/situations faced by travelers, and each situation may occur during a time interval in the morning peak. The six situations and the corresponding equilibrium departure rates will be presented and discussed in the next section.

It is noteworthy that the six equilibrium departure rates (under the abovementioned six situations) are also illustrated in Lindsey (1994) under a binary distribution of bottleneck capacity, but without specifying what commuters experience in these situations. Xiao et al. (2015) explicitly modeled four of these six situations. Long et al. (2022) considered all the six situations, but they considered a continuous distribution rather than a "mixed" capacity distribution in the current paper.

Table 1. Types of schedule delay and queuing experienced by commuters in the stochastic bottleneck model.

Type of schedule delay experience	Type of queuing experience
experience Schedule Delay Early (SDE)	Always experience Queuing (AQ)
possibly experience Schedule Delay either Early or Late (SDE/L)	Possibly experience Queuing (PQ)
experience Schedule Delay Late (SDL)	

2.2 User Equilibrium under stochastic bottleneck capacity

2.2.1 Equilibrium departure rates

Six situations associated with schedule delay and queuing experience faced by the commuters are summarized in Section 2.1. The equilibrium departure rate at each situation and how these departure rates change with π, θ_1 and θ_2 are summarized in Table 2. Detailed derivations of departure rates are omitted here to save space, which are similar to those in Liu et al. (2020). $T(t)$, $R(t)$, t_s and t^* denote the queuing time at time *t*, cumulative departure at time *t*, the first departure time, and the work start time, respectively, and the realized capacity denoted as *s* is a random variable (fluctuates from day to day). Then, we have **Remark 1**.

Remark 1: *When the queuing time* $T(t) = R(t)/s - (t - t_s) > 0$ *i.e.,* $s < R(t)/(t - t_s)$*, commuters departing at time t experience queuing. When* $T(t) + t = R(t)/s - (t - t_s) + t < t^*$*, i.e.,* $s > R(t)/(t^* - t_s)$*, commuters experience schedule delay early with queuing. When* $T(t) + t = R(t)/s - (t - t_s) + t > t^*$*, i.e.,* $s < R(t)/(t^* - t_s)$*, commuters experience schedule delay late with queuing.*

Since there is capacity uncertainty (i.e., the realized capacity varies), whether the commuter arrive early or late and whether they experience queuing depends on the relative magnitude of the realized capacity on a day. The "mixed" capacity distribution involves three critical values, i.e., $\theta_1\bar{s}$, $\theta_2\bar{s}$ and $\bar{s}$. From **Remark 1**, in order to identify the queuing experience for commuters departing at time *t*, one should compare the three critical values against $R(t)/(t - t_s)$. Similarly, the schedule delay experience is obtained by comparing the three critical values with $R(t)/(t^* - t_s)$. Note that commuters departing after t^* always experience schedule delay late regardless of the realized capacity. Different possible situations are given in Table 2, where each may occur during a time interval in the morning peak, and whether one situation will occur or not depends on both the realized capacity and the cumulative departure.

In Table 2, situation S1 (i.e., SDE+AQ) related to "experiencing schedule delay early" (SDE) and "always experience queuing" (AQ) is the same as those in Xiao et al., (2015) and Long et al., (2022). So is situation S3 (i.e., SDL+AQ). However, situations related to "possibly experience schedule delay either early or late" (SDE/L) and/or "possibly experience queuing" (PQ) can be further classified into more sub-situations (subject to the "mixed" capacity distribution considered in this paper). This is because, the "mixed" capacity distribution is more complex (e.g., involves three critical values, i.e., $\theta_1\bar{s}$, $\theta_2\bar{s}$ and $\bar{s}$) than a binary or a continuous distribution (e.g., involves two critical values: the maximum and minimum capacities). This will lead to the possibility of additional equilibrium departure/arrival patterns.

We now take the situations of SDE/L and PQ as examples to further clarify the above. During the peak, consider that the departure/arrival are both continuous over time. For the situations of SDE/L, the capacity $R(t)/(t^* - t_s)$ may be either larger than the upper bound of the degraded capacity, i.e., $R(t)/(t^* - t_s) > \theta_2\bar{s}$, or smaller than the upper bound, i.e., $R(t)/(t^* - t_s) < \theta_2\bar{s}$. It follows that there are two sub-situations: (i) For the former, commuters arrive early if the realized capacity $s = \bar{s}$, otherwise they arrive late; (ii) For the latter, commuters arrive late if capacity degradation occurs and the realized capacity $s < R(t)/(t^* - t_s)$, otherwise they arrive early. Similarly, for the situations of PQ, there are also two sub-situations: (i) when $R(t)/(t - t_s) > \theta_2\bar{s}$, commuters do not experience queuing if the realized capacity $s = \bar{s}$, otherwise they experience queuing; (ii) when $R(t)/(t - t_s) < \theta_2\bar{s}$, commuters experience queuing if capacity degradation occurs and the realized capacity $s < R(t)/(t - t_s)$, otherwise they do not experience any queuing.

Note that subscripts and superscripts of the departure rates in Table 2 are used to indicate the specific situation and the specific sub-situation, respectively. Moreover, the equilibrium departure rates in some sub-situations are time-dependent. All departure rates are positive. The arrows "↑" and "↓" in Table 2 are used to indicate that the departure rates increase and decrease with respect to the parameter in concern, respectively.

Table 2. Possible situations and sub-situations faced by travelers and corresponding departure rates in the stochastic bottleneck model.

Situations	Sub-situations	Departure rates	π	θ_1	θ_2
S1 SDE+AQ	-	$r_1 = \frac{\alpha(\theta_2-\theta_1)\bar{s}}{(\alpha-\beta)\left[\pi\, ln\frac{\theta_2}{\theta_1}+(1-\pi)(\theta_2-\theta_1)\right]}$	↓	↑	↑
S2 SDE/L+AQ	S2-1 $\frac{R(t)}{t^*-t_s} \le \theta_2\bar{s}$	$r_2^1(t) = \frac{\alpha(\theta_2-\theta_1)\bar{s}}{\pi\left[(\alpha-\beta)\, ln\left(\theta_2\bar{s}/\left(\frac{R(t)}{t^*-t_s}\right)\right)+(\alpha+\gamma)\left(ln\frac{R(t)}{(t^*-t_s)\theta_1\bar{s}}\right)\right]+(1-\pi)(\alpha-\beta)(\theta_2-\theta_1)}$	↓	↑	↑
	S2-2 $\frac{R(t)}{t^*-t_s} > \theta_2\bar{s}$	$r_2^2 = \frac{\alpha(\theta_2-\theta_1)\bar{s}}{\pi(\alpha+\gamma)\, ln\frac{\theta_2}{\theta_1}+(1-\pi)(\alpha-\beta)(\theta_2-\theta_1)}$	↓	↑	↑
S3 SDL+AQ	-	$r_3 = \frac{\alpha(\theta_2-\theta_1)\bar{s}}{(\alpha+\gamma)\left[\pi\, ln\frac{\theta_2}{\theta_1}+(1-\pi)(\theta_2-\theta_1)\right]}$	↓	↑	↑
S4 SDL+PQ	S4-1 $\frac{R(t)}{t-t_s} \ge \theta_2\bar{s}$	$r_4^1 = \frac{[\pi\alpha-(1-\pi)\gamma](\theta_2-\theta_1)\bar{s}}{\pi(\alpha+\gamma)\, ln\frac{\theta_2}{\theta_1}}$	↑	↑	↑
	S4-2 $\frac{R(t)}{t-t_s} < \theta_2\bar{s}$	$r_4^2(t) = \frac{\pi(\alpha+\gamma)\left(\frac{R(t)}{t-t_s}-\theta_1\bar{s}\right)-\gamma(\theta_2-\theta_1)\bar{s}}{\pi(\alpha+\gamma)\left(ln\frac{R(t)}{t-t_s}-ln\,\theta_1\bar{s}\right)}$	↑	indeterminate	↓
S5 SDE/L+PQ	S5-1 $\frac{R(t)}{t^*-t_s} < \theta_2\bar{s} < \frac{R(t)}{t-t_s}$	$r_5^1(t) = \frac{[\pi\alpha+(1-\pi)\beta](\theta_2-\theta_1)\bar{s}}{\pi(\alpha-\beta)\left(ln\,\theta_2\bar{s}-ln\frac{R(t)}{t^*-t_s}\right)+\pi(\alpha+\gamma)\left(ln\frac{R(t)}{t^*-t_s}-ln\,\theta_1\bar{s}\right)}$	↓	↑	↑
	S5-2 $\frac{R(t)}{t^*-t_s} < \frac{R(t)}{t-t_s} < \theta_2\bar{s}$	$r_5^2(t) = \frac{\pi(\alpha-\beta)\left(\frac{R(t)}{t-t_s}-\theta_1\bar{s}\right)+\beta(\theta_2-\theta_1)\bar{s}}{\pi(\alpha+\gamma)\left(ln\frac{R(t)}{t^*-t_s}-ln\,\theta_1\bar{s}\right)+\pi(\alpha-\beta)\left(ln\frac{R(t)}{t-t_s}-ln\frac{R(t)}{t^*-t_s}\right)}$	↓	indeterminate	↑
	S5-3 $\theta_2\bar{s} < \frac{R(t)}{t^*-t_s} < \frac{R(t)}{t-t_s}$	$r_5^3 = \frac{[\pi\alpha+(1-\pi)\beta](\theta_2-\theta_1)\bar{s}}{\pi(\alpha+\gamma)\, ln\frac{\theta_2}{\theta_1}}$	↓	↑	↑
S6 SDE+PQ	S6-1 $\frac{R(t)}{t-t_s} \ge \theta_2\bar{s}$	$r_6^1 = \frac{[\pi\alpha+(1-\pi)\beta](\theta_2-\theta_1)\bar{s}}{\pi(\alpha-\beta)\, ln\frac{\theta_2}{\theta_1}}$	↓	↑	↑
	S6-2 $\frac{R(t)}{t-t_s} < \theta_2\bar{s}$	$r_6^2 = \frac{\pi(\alpha-\beta)\left(r_6^2-\theta_1\bar{s}\right)+\beta(\theta_2-\theta_1)\bar{s}}{\pi(\alpha-\beta)\left(ln\, r_6^2-ln\,\theta_1\bar{s}\right)}$	↓	indeterminate	↑

From Table 2, we further have the following observations. The departure rates decrease with respect to π except those in S4, while they increase with respect to θ_2 except those in S4-2. Also, the departure rates increase with respect to θ_1 except the situation-dependency for S4-2, S5-2 and S6-2. The increase of π or the decreases of θ_1 and θ_2 indicates that the adverse conditions (negative impacts on capacity) occur more frequently or the capacity becomes smaller under adverse conditions. Thus, the equilibrium departure rates (in general) decrease. However, the departure rates increase with respect to π in S4 and they decrease with respect to θ_2 in S4-2. This is because, the number of commuters departing after work start time per unit time will be larger to avoid being heavily penalized by the large penalty of arriving late when the capacity distribution becomes less favorable.

2.2.2 Equilibrium departure/arrival patterns

Due to the "mixed" capacity distribution and the resulting complex situations and sub-situations defined in Table 2, there are multiple equilibrium departure/arrival patterns, depending on all the parameters involved. To facilitate reading, we organize these departure/arrival patterns as follows. (i) For those departure/arrival profiles involving the same group of situations defined in Table 2, we group them as one pattern, i.e., six possible equilibrium departure/arrival patterns (Patterns 1-6) in Table 3. (ii) For the same pattern (with the same group of situations), there can be different sub-situations (also defined in Table 2). Depending on the combination of sub-situations, we define sub-patterns (see Table 3).

Pattern 1 and Pattern 4 are similar to those in Lindsey (1994) where a binary capacity distribution is assumed, while both patterns in this study now involve sub-situations due to a more complex capacity distribution. Patterns 2, 3, 5 and 6 all involve sub-patterns.

We have the following observations from Table 3. Firstly, the six situations defined in Table 2 cannot simultaneously appear in one departure/arrival pattern (at most four situations can co-exist in one pattern). Moreover, "always queuing" (AQ) must occur before "possibly queuing" (PQ). And "schedule delay early" (SDE) always occur before "schedule delay late" (SDL) and "possibly schedule delay early or late" (SDE/L) will occur in between. Finally, either S1 or S6 will occur first (over clock time), since the first commuter always arrives early. The last situations to occur (over clock time) in Patterns 1-3 are identical, the last situations in Patterns 5a, 6a and 6b are identical, and the last situations in Patterns 5b, 5c and 6c are identical.

Table 3. Possible equilibrium departure/arrival patterns in the stochastic bottleneck model.

Pattern	Situations	Sub-pattern	Situations and sub-situations
1	S1, S2, S3, S4	1	S1, S2-1, S2-2, S3, S4-1, S4-2
2	S1, S2, S5, S4	2a	S1, S2-1, S5-1, S5-2, S4-2
		2b	S1, S2-1, S5-1, S5-3, S4-1, S4-2
		2c	S1, S2-1, S2-2, S5-3, S4-1, S4-2
3	S6, S5, S4	3a	S6-2, S5-2, S4-2
		3b	S6-1, S5-1, S5-2, S4-2
		3c	S6-1, S5-1, S5-3, S4-1, S4-2
4	S1, S2, S3	4	S1, S2-1, S2-2, S3
5	S1, S2, S5	5a	S1, S2-1, S5-1, S5-2
		5b	S1, S2-1, S5-1, S5-3
		5c	S1, S2-1, S2-2, S5-3
6	S6, S5	6a	S6-2, S5-2
		6b	S6-1, S5-1, S5-2
		6c	S6-1, S5-1, S5-3

As illustrated in Figures 1-6, we let t_j^i denote the j-th critical time point defined for Pattern i, where before and after this point the departure rates differ (corresponding to different situations defined in Table 2). t_s, t^* and t_e denote the earliest departure time, the work start time and the latest departure time, respectively.

We now discuss Pattern 1 in detail as an example to show how the equilibrium pattern can be derived. Pattern 1 in Figure 1 involves situations/sub-situations S1, S2-1, S2-2, S3, S4-1 and S4-2. The corresponding departure rates are r_1, $r_2^1(t)$, r_2^2, r_3, r_4^1 and $r_4^2(t)$, respectively.

(i) The first situation to occur (over clock time) is S1 within the time interval (t_s, t_1^1). Commuters departing at the time interval always experience schedule delay early and queuing regardless of the realization of capacity, as shown in Figure 1. From **Remark 1**, the conditions $R(t)/(t^* - t_s) < \theta_1\bar{s} < \theta_2\bar{s} < \bar{s} < R(t)/(t - t_s)$ are met in situation S1.

(ii) The second situation is S2-1 that occurs within the time interval (t_1^1, t_2^1). For situation S2-1, we should have the conditions $\theta_1\bar{s} < R(t)/(t^* - t_s) < \theta_2\bar{s} < \bar{s} < R(t)/(t - t_s)$ hold for $R(t)$, since $R(t)$ increases continuously over time. Note that the condition $\theta_1\bar{s} < \theta_2\bar{s} < R(t)/(t^* - t_s) < \bar{s} < R(t)/(t - t_s)$ cannot occur immediately after that for S1 ($R(t)/(t^* - t_s) < \theta_1\bar{s} < \theta_2\bar{s} < \bar{s} < R(t)/(t - t_s)$), otherwise the cumulative departure is not continuous.

For situation S2-1, commuters always experience queuing regardless of the realized capacity. They arrive late when the degraded condition occurs and the realized capacity $s < R(t)/(t^* - t_s)$, otherwise they arrive early.

For the critical time point t_1^1, commuters departing at t_1^1 arrive at t^* when the realized capacity is the minimum one, i.e., $\theta_1\bar{s}$, as shown in Figure 1. From the condition of situation S1 and S2-1, we can also obtain that the cumulative departures at t_1^1 should satisfy $R(t_1^1) = \theta_1\bar{s}(t^* - t_s)$. Then, the expected travel cost at t_1^1 can be obtained by substituting $R(t_1^1)$ into $E\big(C(t_1^1)\big)$. At equilibrium, we have $E\big(C(t_1^1)\big) = \beta(t^* - t_s)$, since the first commuter only experiences schedule delay early cost without queuing. Therefore, t_1^1 can be derived as an expression of t_s.

(iii) The next situation is S2-2 within the time interval (t_2^1, t_3^1). The condition $\theta_1\bar{s} < \theta_2\bar{s} <$

$R(t)/(t^* - t_s) < \bar{s} < R(t)/(t - t_s)$ is satisfied in S2-2. Commuters departing during the time interval always experience queuing regardless of the realized capacity. They arrive early when the realized capacity is the designed one, otherwise they arrive late. From the conditions of situation S2-1 and S2-2, the cumulative departures at t_2^1 can be given as $R(t_2^1) = \theta_2\bar{s}(t^* - t_s)$. Similar to the above, t_2^1 can also be formulated as an expression of t_s.

(iv) The following situation is S3 within the time interval (t_3^1, t_4^1). The condition $\theta_1\bar{s} < \theta_2\bar{s} < \bar{s} < R(t)/(t^* - t_s) < R(t)/(t - t_s)$ is satisfied in S3. Commuters departing during the time interval always experience queuing and arrive late regardless of the realized capacity. The cumulative departures at t_3^1 is $R(t_3^1) = \bar{s}(t^* - t_s)$, and t_3^1 can be formulated as a function of t_s.

(v) The next situation is S4-1 within the time interval (t_4^1, t_5^1). The condition $\theta_1\bar{s} < \theta_2\bar{s} < R(t)/(t - t_s) < \bar{s} < R(t)/(t^* - t_s)$ is satisfied in S4-1. Commuters departing during the time interval always arrive late regardless of the realized capacity. They do not experience queuing when the realized capacity is the designed one, otherwise they experience queuing. The cumulative departures at t_4^1 is $R(t_4^1) = \bar{s}(t_4^1 - t_s)$, and t_4^1 can be formulated as a function of t_s.

Note that as the situation changes from S3 (always queuing) to S4-1 (possibly queuing) over time, the cumulative departures change from $R(t) > \bar{s}(t - t_s)$ to $R(t) < \bar{s}(t - t_s)$. This indicates that while the cumulative departures are increasing, the expected queue length is dissipating.

(vi) The last situation is S4-2 within the time interval (t_5^1, t_e). The condition $\theta_1\bar{s} < R(t)/(t - t_s) < \theta_2\bar{s} < \bar{s} < R(t)/(t^* - t_s)$ is satisfied in S4-2. Commuters departing at the time interval always arrive late regardless of the realized capacity. They experience queuing when the degraded condition occurs and the realized capacity $s < R(t)/(t - t_s)$, otherwise they do not experience queuing. The cumulative departures at t_5^1 is $R(t_5^1) = \theta_2\bar{s}(t_5^1 - t_s)$, and t_5^1 can be formulated as a function of t_s.

At equilibrium, condition $E\big(C(t_e)\big) = \beta(t^* - t_s)$ is satisfied. From the equilibrium condition, the earliest and latest departure times depend on the last situation of each pattern. Therefore, the earliest and latest departure times under departure/arrival patterns with the same last situation have identical formulations (if the numerical parameters in the formulations are the same, these time points will be identical). Correspondingly, the earliest and latest departure times under Patterns 1-3 have identical formulations, those under Patterns 5a, 6a and 6b have identical formulations, and those under Patterns 5b, 5c and 6c have identical formulations.

The latest departure time is after t^* in Patterns 1-3. Also, the departure rate at $t = t_e$ should be zero, i.e., $r_4^2(t_e) = 0$. Otherwise, travelers will adjust their departure times to those after t_e to attain lower travel cost until the departure rate of the latest departure time is zero. The condition ensures that the equilibrium is achieved where the departure rate (after t^*) is positive. Note that the departure rate does not drop to zero if the probability distribution of capacity is discrete, as assumed in studies that employ two-point distributions (Lindsey, 1994; Liu et al., 2020). Then the first and the latest departure times can be obtained accordingly based on the equilibrium conditions in Patterns 1-3. From Figure 4, $t_e - t_s = N/\bar{s}$ is satisfied in Pattern 4 since commuters always experiencing queuing. For Patterns 5-6, the latest departure time $t_e = t^*$, as shown in Figures 5 and 6. Combining with the equilibrium condition, i.e., $E\big(C(t_e)\big) = \beta(t^* - t_s)$, t_s and t_e can also be obtained in Patterns 4-6.

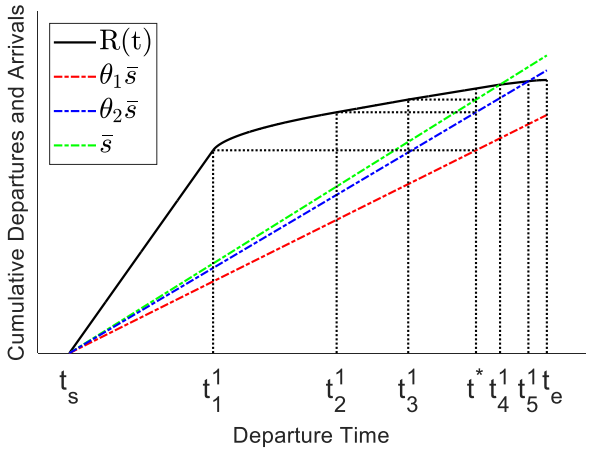

Figure 1. Equilibrium departure/arrival pattern: Pattern 1.

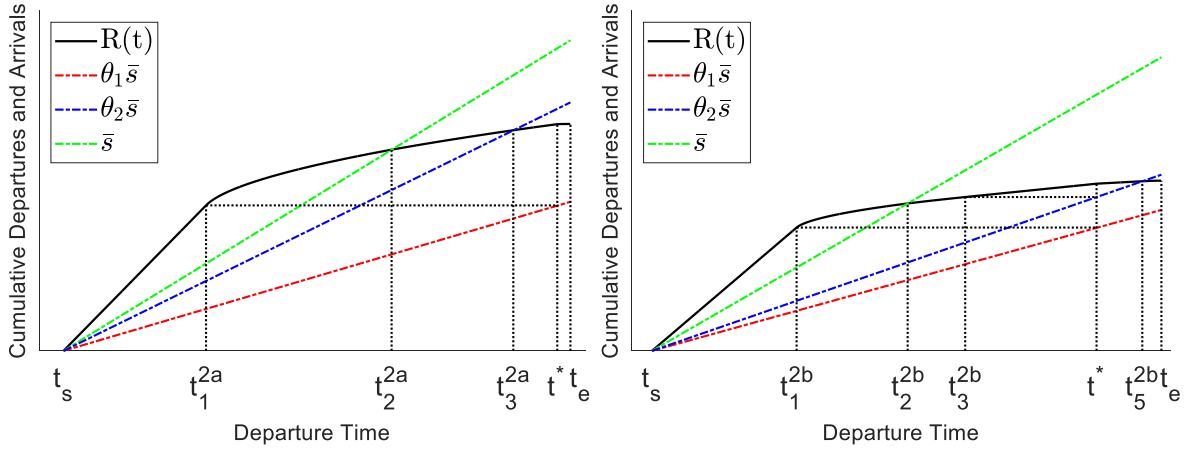

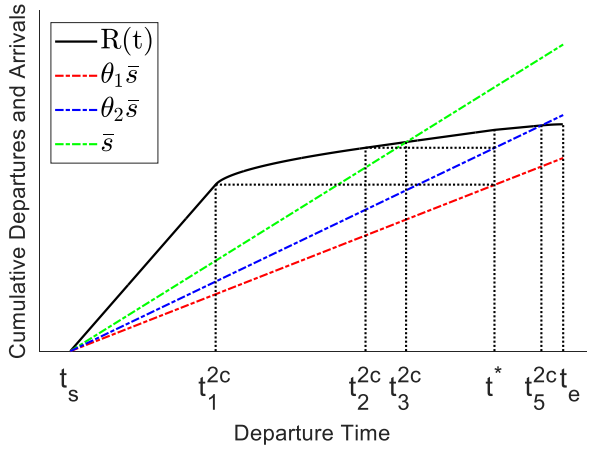

(c)

Figure 2. Equilibrium departure/arrival patterns: (a) Pattern 2a, (b) Pattern 2b, (c) Pattern 2c.

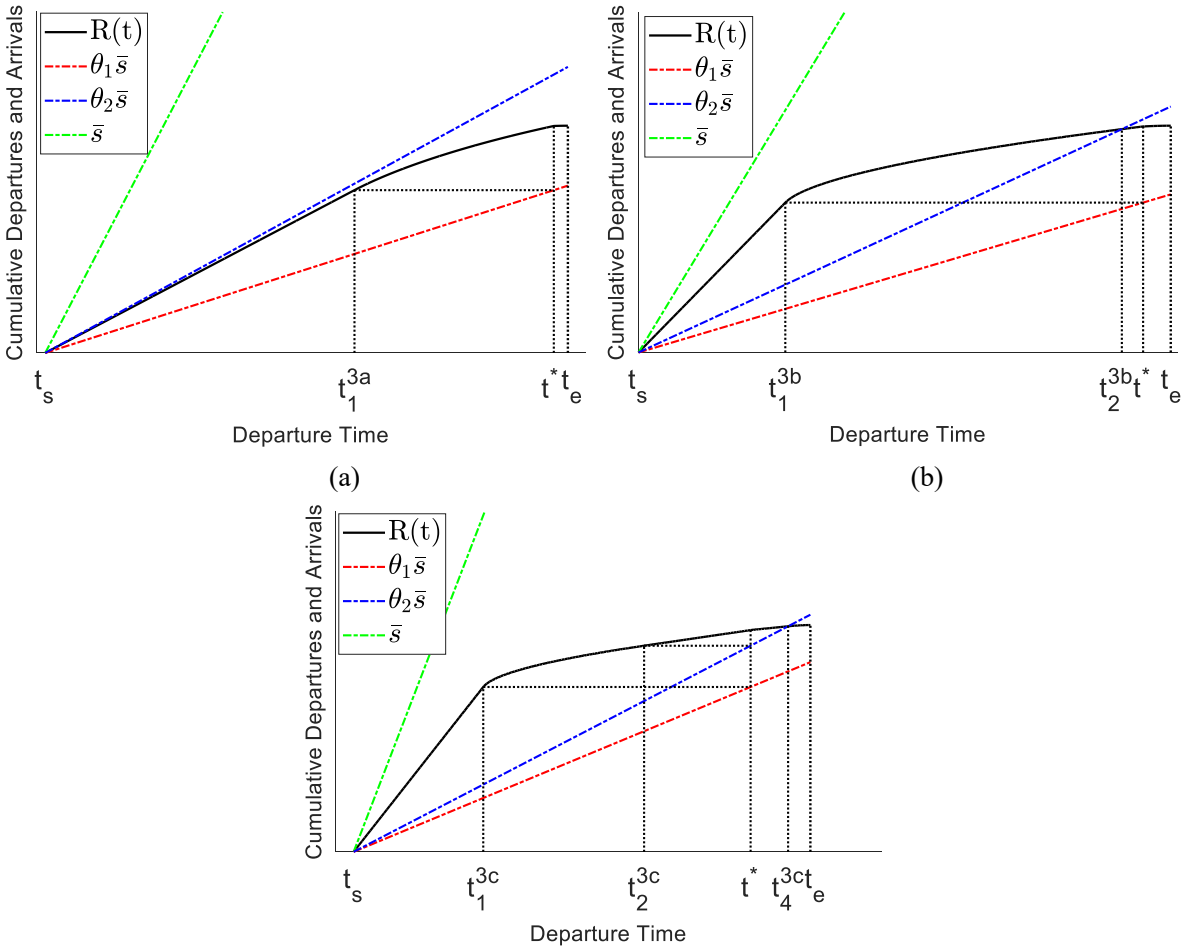

Figure 3. Equilibrium departure/arrival patterns: (a) Pattern 3a, (b) Pattern 3b, (c) Pattern 3c.

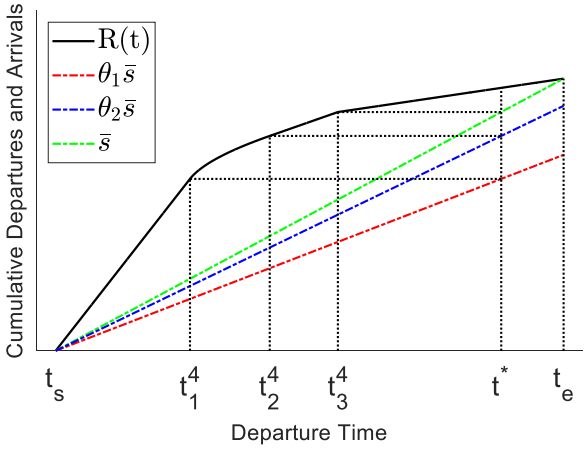

Figure 4. Equilibrium departure/arrival pattern: Pattern 4.

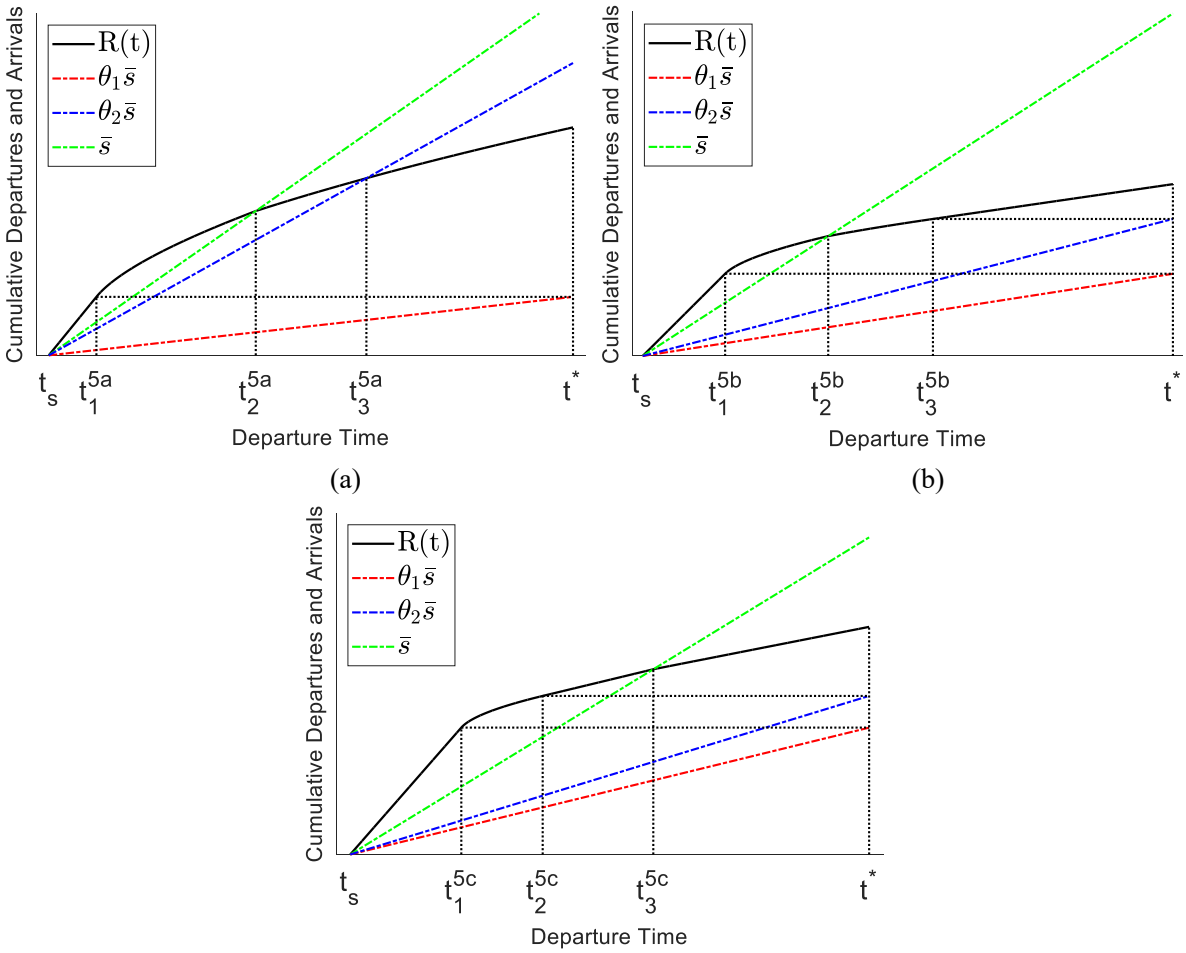

Figure 5. Equilibrium departure/arrival patterns: (a) Pattern 5a, (b) Pattern 5b, (c) Pattern 5c.

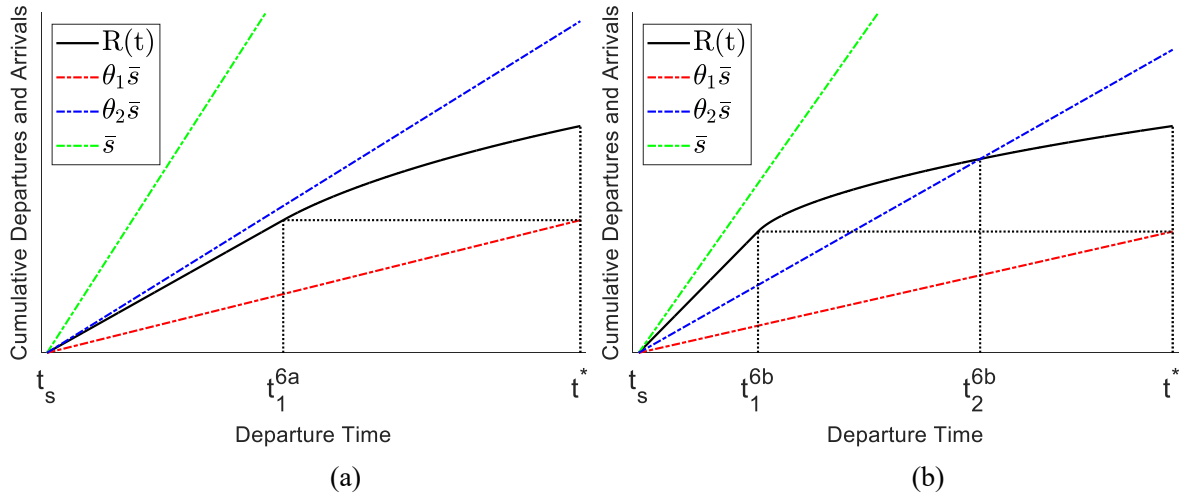

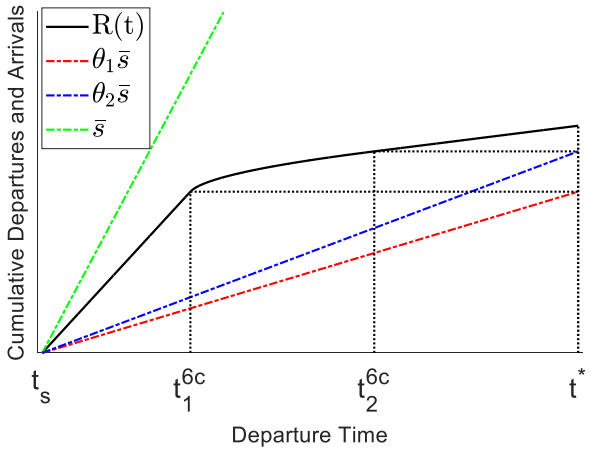

(c)

Figure 6. Equilibrium departure/arrival patterns: (a) Pattern 6a, (b) Pattern 6b, (c) Pattern 6c.

The first and latest departure time points (of commuters) and other critical time points for different equilibrium departure/arrival patterns (as indicated in Figures 1-6) are given in Table 4 and Table 5, respectively. The detailed derivations are given in Appendix A (online appendix).

As shown in Table 4, let $\hat{s}$ be the smallest (realized) capacity at which the last commuter departing at t_e can avoid queuing, and we have $\hat{s} = N/(t_e - t_s)$. We then can derive that $\hat{s} = \theta_1\bar{s} + (\gamma(\theta_2 - \theta_1)\bar{s})/\big(\pi(\alpha+\gamma)\big)$ for Patterns 1-3; $\hat{s} = \bar{s}$ in Pattern 4; and $\hat{s}$ solves the equality $\hat{s}\,ln(\hat{s}/\theta_1\bar{s}) - \hat{s} = (\beta(\theta_2 - \theta_1)\bar{s})/\big(\pi(\alpha+\gamma)\big) - \theta_1\bar{s}$ for Patterns 5a, 6a and 6b; and $\hat{s} = \big[\beta/\big(\pi(\alpha+\gamma)\big) + 1\big]\big((\theta_2 - \theta_1)\bar{s}\big)/(ln\,\theta_2 - ln\,\theta_1)$ for Patterns 5b, 5c and 6c. Note that for Pattern 4 commuters always experience queuing unless $\hat{s} = \bar{s}$. Differently, we have $\theta_1\bar{s} < \hat{s} < \theta_2\bar{s}$ for Patterns 1-3, 5a, 6a and 6b, and $\theta_2\bar{s} < \hat{s} < \bar{s}$ for Patterns 5b, 5c and 6c.

Table 4. The first and latest departure time points under different equilibrium departure/arrival patterns.

Pattern	The first departure time point (t_s)	The latest departure time point (t_e)
1-3	$t^* - \frac{N}{\hat{s}(\beta+\gamma)}\left[\frac{\pi(\alpha+\gamma)\left(\hat{s}\,ln\frac{\hat{s}}{\theta_1\bar{s}} - (\hat{s}-\theta_1\bar{s})\right)}{(\theta_2-\theta_1)\bar{s}} + \gamma\right]$	$t^* + \frac{N}{\hat{s}(\beta+\gamma)}\left[\beta - \frac{\pi(\alpha+\gamma)\left(\hat{s}\,ln\frac{\hat{s}}{\theta_1\bar{s}} - (\hat{s}-\theta_1\bar{s})\right)}{(\theta_2-\theta_1)\bar{s}}\right]$
4	$t^* - \frac{N}{\bar{s}(\beta+\gamma)}\left[\pi(\alpha+\gamma)\left(\frac{ln\,\theta_2 - ln\,\theta_1}{\theta_2-\theta_1} - 1\right) + \gamma\right]$	$t^* + \frac{N}{\bar{s}(\beta+\gamma)}\left[\beta - \pi(\alpha+\gamma)\left(\frac{ln\,\theta_2 - ln\,\theta_1}{\theta_2-\theta_1} - 1\right)\right]$
5-6	$t_s = t^* - \frac{N}{\hat{s}}$	t^*

As can be seen from Table 5, the closed form solutions of some critical time points are not available. These critical time points depend on $E\big(C(t)\big)$, i.e., the expected travel cost at these time points. As the departure rates are nonlinear (as shown in Table 2), closed form solutions are not always available (due to nonlinear equations). The corresponding nonlinear equations used to solve the critical time points are given in Appendix A (online appendix). Table 5 summarizes the equation numbers. The equilibrium solutions of these equations are unique, and Appendix A also provides the proofs. These nonlinear equations can be solved by the Newton's method numerically.

Other equilibrium departure/arrival patterns can be identified and solved in a similar way and discussions of them are omitted here to save space.

Table 5. Critical time points under different equilibrium departure/arrival patterns (Note: $\hat{t} = t^* - t_s$, $\Theta = \frac{1}{\theta_2 - \theta_1} ln \frac{\theta_2}{\theta_1}$, and $\varphi = \pi(\alpha + \gamma)(\Theta - 1)$).

Pattern	Time point 1	Time point 2	Time point 3	Time point 4	Time point 5
1	$t_1^1 = t^* - \frac{\alpha - \theta_1(\alpha-\beta)[1+\pi(\Theta-1)]}{\alpha}\hat{t}$	$t_2^1 = t^* - \frac{\alpha - \theta_2(\varphi+\alpha-\beta)+\pi(1-\theta_2)(\beta+\gamma)}{\alpha}\hat{t}$	$t_3^1 = t^* - \frac{\beta-\varphi}{\alpha}\hat{t}$	$t_4^1 = t^* + \frac{\beta-\varphi}{\varphi+\gamma}\hat{t}$	$t_5^1 = t^* + \frac{\beta-\pi(\alpha+\gamma)(\theta_2\Theta-1)}{\pi(\alpha+\gamma)(\theta_2\Theta-1)+\gamma}\hat{t}$
2a	$t_1^{2a} = t_1^1$	t_2^{2a} solves Eq. (A.10)	t_3^{2a} solves Eq. (A.11)	$t_4^{2a} = t^*$	-
2b	$t_1^{2b} = t_1^1$	$t_2^{2b} = t_2^{2a}$	$t_3^{2b} = t^* - \frac{\pi(\alpha+\gamma)(1-\theta_2\theta)+\beta}{\pi(\alpha-\beta)+\beta}\hat{t}$	$t_4^{2b} = t^*$	$t_5^{2b} = t_5^1$
2c	$t_1^{2c} = t_1^1$	$t_2^{2c} = t_2^1$	$t_3^{2c} = t^* - \frac{\varphi-\beta}{\varphi+\pi(\beta+\gamma)-\beta}\hat{t}$	$t_4^{2c} = t^*$	$t_5^{2c} = t_5^1$
3a	$t_1^{3a} = t^* - \left(1 - \frac{\theta_1\bar{s}}{r_6^2}\right)\hat{t}$	$t_2^{3a} = t^*$	-	-	-
3b	$t_1^{3b} = t^* - \left(1 - \frac{\pi(\alpha-\beta)\theta_1\theta}{\pi(\alpha-\beta)+\beta}\right)\hat{t}$	$t_2^{3b} = t_3^{2a}$	$t_3^{3b} = t^*$	-	-
3c	$t_1^{3c} = t_1^{3b}$	$t_2^{3c} = t_3^{2b}$	$t_3^{3c} = t^*$	$t_4^{3c} = t_5^1$	-
4	$t_1^4 = t^* - \frac{\alpha - \theta_1(\alpha-\beta)[1+\pi(\Theta-1)]}{\alpha}\hat{t}$	$t_2^4 = t^* - \frac{\alpha - \theta_2(\varphi+\alpha-\beta)+\pi(1-\theta_2)(\beta+\gamma)}{\alpha}\hat{t}$	$t_3^4 = t^* - \frac{\beta-\varphi}{\alpha}\hat{t}$	-	-
5a	$t_1^{5a} = t^* - \frac{\alpha - \theta_1(\alpha-\beta)[1+\pi(\Theta-1)]}{\alpha}\hat{t}$	t_2^{5a} solves Eq. (A.10)	t_3^{5a} solves Eq. (A.11)	-	-
5b	$t_1^{5b} = t_1^{5a}$	$t_2^{5b} = t_2^{5a}$	$t_3^{5b} = t^* - \frac{\pi(\alpha+\gamma)(1-\theta_2\theta)+\beta}{\pi(\alpha-\beta)+\beta}\hat{t}$	-	-
5c	$t_1^{5c} = t_1^{5a}$	$t_2^{5c} = t^* - \frac{\alpha - \theta_2(\varphi+\alpha-\beta)+\pi(1-\theta_2)(\beta+\gamma)}{\alpha}\hat{t}$	$t_3^{5c} = t^* - \frac{\varphi-\beta}{\varphi+\pi(\beta+\gamma)-\beta}\hat{t}$	-	-
6a	$t_1^{6a} = t^* - \left(1 - \frac{\theta_1\bar{s}}{r_6^2}\right)\hat{t}$	-	-	-	-
6b	$t_1^{6b} = t^* - \left(1 - \frac{\pi(\alpha-\beta)\theta_1\theta}{\pi\alpha+(1-\pi)\beta}\right)\hat{t}$	$t_2^{6b} = t_3^{5a}$	-	-	-
6c	$t_1^{6c} = t_1^{6b}$	$t_2^{6c} = t_3^{5b}$	-	-	-

In Table 6, the boundary conditions for occurrence of the six possible equilibrium departure/arrival patterns listed in Table 3 are summarized. The detailed derivations of these conditions are given in Appendix B (online appendix). To facilitate the presentation, we introduce the following parameters: $\pi_C = \gamma/(\alpha+\gamma)$; $\pi_S = \beta/[(\alpha+\gamma)(\Theta-1)]$; $\pi_R = \beta/[(\alpha+\gamma)(\theta_2\Theta-1)]$; $\pi_N = \beta/[(\alpha-\beta)(\Theta-1)]$; $\pi_M = \beta/[(\alpha-\beta)(\theta_2\Theta-1)]$; $\pi_L = \beta/[(\alpha+\gamma)\Theta-(\alpha-\beta)-(\beta+\gamma)/\theta_2]$ and $\pi_T = \big(\gamma(\theta_2-\theta_1)\big)/(\theta_1(\alpha+\gamma)\chi)$, where $\Theta = (ln\theta_2 - ln\theta_1)/(\theta_2-\theta_1)$, and χ is defined as the solution of non-linear equation $(1+1/\chi)\,ln(1+\chi) = (\beta+\gamma)/\gamma$. One can verify that $\pi_N > \pi_S$, $\pi_M > \pi_R$, $\pi_R > \pi_L > \pi_S$ and $\pi_M > \pi_N > \pi_L$ hold. In the numerical studies, we will further illustrate how these boundary conditions vary graphically.

Table 6. Boundary conditions for occurrence of different equilibrium departure/arrival patterns.

Pattern	Condition
1	$\pi_C \le \pi < \pi_S$
2a	$max\{\pi_C,\pi_R,\pi_T\} < \pi < \pi_N$
2b	$max\{\pi_C,\pi_L,\pi_T\} < \pi < min\{\pi_R,\pi_N\}$
2c	$max\{\pi_C,\pi_S,\pi_T\} < \pi < \pi_L$
3a	$\pi > max\{\pi_C,\pi_M,\pi_T\}$
3b	$max\{\pi_C,\pi_N,\pi_R,\pi_T\} < \pi < \pi_M$
3c	$max\{\pi_C,\pi_N,\pi_T\} < \pi < \pi_R$
4	$\pi < min\{\pi_C,\pi_S\}$
5a	$max\{\pi_C,\pi_R\} < \pi < min\{\pi_N,\pi_T\}$ or $\pi_R \le \pi < min\{\pi_C,\pi_N\}$
5b	$max\{\pi_C,\pi_L\} < \pi < min\{\pi_R,\pi_N,\pi_T\}$ or $\pi_L \le \pi < min\{\pi_R,\pi_N,\pi_C\}$
5c	$max\{\pi_C,\pi_S\} < \pi < min\{\pi_L,\pi_T\}$ or $\pi_S \le \pi < min\{\pi_L,\pi_C\}$
6a	$max\{\pi_C,\pi_M\} < \pi \le \pi_T$ or $\pi_M \le \pi < \pi_C$
6b	$max\{\pi_C,\pi_N,\pi_R\} < \pi < min\{\pi_M,\pi_T\}$ or $max\{\pi_N,\pi_R\} < \pi < min\{\pi_C,\pi_M\}$
6c	$max\{\pi_C,\pi_N\} < \pi < min\{\pi_T,\pi_R\}$ or $\pi_N \le \pi < min\{\pi_C,\pi_R\}$

3. Properties of equilibrium patterns

This section examines the properties of the equilibrium patterns. To this end, we analyze the impacts of different parameters on two important efficiency metrics, i.e., the individual mean travel cost, denoted as $E(C)$, and the mean of total travel time of all commuters, denoted as $E(TT)$ under each pattern. As mentioned in Section 2.2, the earliest and latest departure times under Patterns 1-3 have identical formulations, those under Patterns 5a, 6a and 6b have identical formulations, and those under Patterns 5b, 5c and 6c have identical formulations. At the equilibrium, mean travel cost $E(C) = \beta(t^* - t_s)$, and $E(C)$ under the corresponding patterns also has identical formulations. Note that due to complex formulations of $E(C)$ under Patterns 5a, 6a and 6b, some results cannot be analytically verified under these patterns, so some results are based on extensive numerical evaluations.

We list the related findings that have been numerically verified as "Numerical findings" (based on extensive numerical studies where we vary the numerical settings but did not find any counterexample). For the results that can be rigorously proved, we list them in the "Propositions". Note that we also present some numerical examples to illustrate the findings. To facilitate the reading, the proofs of the propositions

are all relayed to Appendix C (online appendix). Moreover, we list some numerical facts in the "Remarks".

For the numerical example, the benchmark numerical settings are given as follows. We adopt the capacity data in empirical study by Qin and Smith (2001). The capacity of 1950 veh/h/lane estimated (for one location) in Qin and Smith (2001) is used as designed capacity for one lane. Therefore, for three-lane road bottleneck the designed capacity is $\bar{s} = 5850$veh/h. The value of time for the peak-period travelers making work-related trips follows $\alpha = 19.72\$/\text{h}$ as estimated in the empirical study by Ozbay and Yanmaz-Tuzel (2008). The ratios β/α=0.61 and γ/α=2.38 estimated by Small (1982) are used, where β and γ are the value of schedule delay early and value of schedule delay late, respectively. The travel demand is assumed as $N = 6000$ veh and the work start time is assumed as $t^* = 9$ h.

Considering the capacity distribution, we firstly investigate the impacts of width of degraded capacity range under the given mean degraded capacity. To facilitate the analysis, we define $e = (\theta_1 + \theta_2)/2$ as the ratio of mean degraded capacity, and $m = \theta_2 - \theta_1$ as the width of degraded capacity range. Under the given mean degraded capacity, i.e., a fixed value of *e*, we have the following results.

Proposition 1. *Under the given e,* $\partial E(C)/\partial m > 0$ *under Patterns 1-4, 5b, 5c and 6c.*

Numerical finding 1. *Under the given e,* $\partial E(C)/\partial m > 0$ *under Patterns 5a, 6a and 6b.*

Remark 2. *Under the given e, whether* $\partial E(TT)/\partial m > 0$ *or* $\partial E(TT)/\partial m < 0$ *depends on the parameters.*

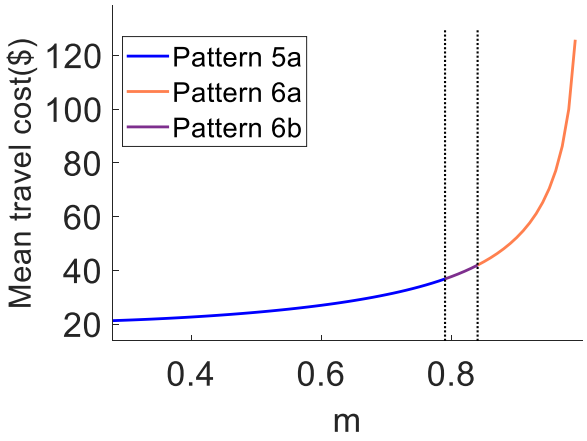

Figure 7. $E(C)$ vs. m. $e = 0.5$, $\pi = 0.9$.

From **Proposition 1**, the mean travel cost increases with the width of degraded capacity range under Patterns 1-4, 5b, 5c and 6c. **Numerical finding 1** indicates that no counterexample is found against the fact under other patterns. A numerical example is presented in Figure 7. Note that the vertical dotted lines in each figure shown in this section and next section are used to indicate different patterns.

Note that for simplicity, in the capacity degraded situations, a binary distribution of capacity is often assumed and degraded capacity range is ignored in the literatures (see, e.g., Lindsey 1994; Lindsey et al., 2014; Liu et al., 2020; Yu et al., 2021). Therefore, given the same mean capacity, the mean travel cost tends to be underestimated if a binary distribution is assumed. The might be partially because that equilibrium costs are increasing and convex with respect to the level of capacity drop. Suppose, for example, that the capacity reduction is uniformly distributed from 0.25 to 0.75, with a mean of 0.5. Relative to a certain reduction of 50 percent, costs increase by more with a 75 percent reduction than they increase by less with a 25 percent reduction. Consequently, the uniform distribution results in higher expected costs.

However, on the other hand, **Remark 2** indicates that the mean of total queueing time is not necessarily underestimated.

An intuitive expectation is that by relieving the capacity degradation, a better system performance can be achieved. Specifically, improving θ_1 and θ_2 can be achieved by, e.g., dispatching emergency vehicles to incident site as soon as possible, or temporarily opening the emergency lane. Improving π can be achieved by, e.g., alerting drivers on the frequent accident sites, or installing more cameras to control overspeed. However, this is not necessarily always the case, as summarized in **Remark 3**.

Proposition 2. *Under Patterns 1-6,* $\partial E(C)/\partial\theta_1 < 0$, $\partial E(C)/\partial\theta_2 < 0$, $\partial E(C)/\partial\pi > 0$.

Remark 3. *Whether* $\partial E(TT)/\partial\rho > 0$ *or* $\partial E(TT)/\partial\rho < 0$ *depends on the parameters, where* $\rho = \theta_1$, θ_2 *and* π.

Proposition 2 indicates that the mean travel cost decreases with the increase of θ_1 and θ_2, and increases with the increase of π. **Remark 3** further indicates that relieving the capacity degradation sometimes might lead to more queueing time. Numerical results demonstrate that when π is relatively small, the total queueing time might increase with the increase of θ_1 and θ_2, and with a relatively small ratio of θ_1/θ_2, the total queueing time might increase with the decrease of π. Under these circumstances, the decrease of average schedule delay cost exceeds the increase of average queueing cost, so that the mean travel cost still decreases.

Proposition 3. *Under Patterns 1-4, 5b, 5c and 6c,* $|\partial E(C)/\partial\theta_1| > |\partial E(C)/\partial\theta_2|$.

Numerical finding 2. *Under Patterns 5a, 6a and 6b,* $|\partial E(C)/\partial\theta_1| > |\partial E(C)/\partial\theta_2|$.

Remark 4. *Whether* $|\partial E(TT)/\partial\theta_1| > |\partial E(TT)/\partial\theta_2|$ *or* $|\partial E(TT)/\partial\theta_1| < |\partial E(TT)/\partial\theta_2|$ *depends on the parameters.*

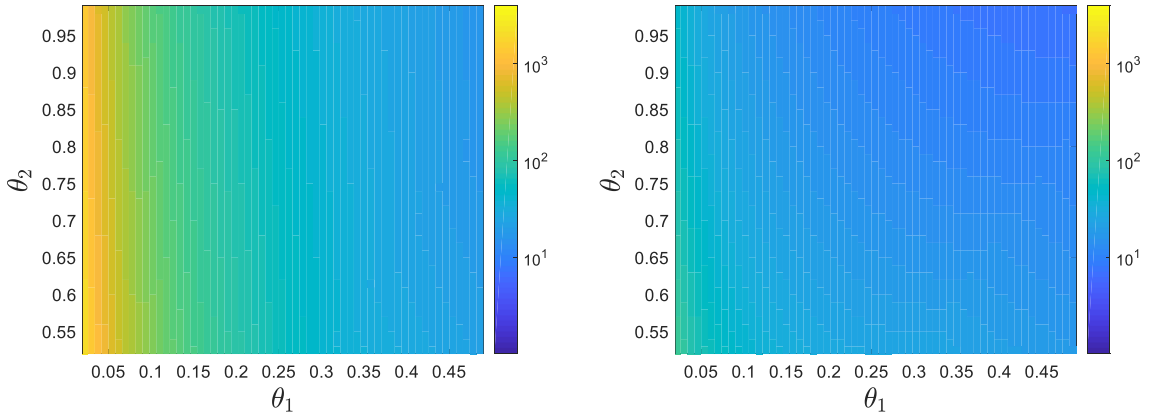

(a) (b)

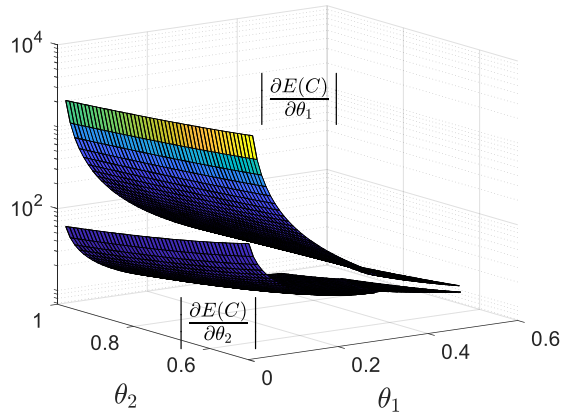

Figure 8. The comparisons of $|\partial E(C)/\partial \theta_1|$ and $|\partial E(C)/\partial \theta_2|$. $\pi = 0.8$. (a) $|\partial E(C)/\partial \theta_1|$; (b) $|\partial E(C)/\partial \theta_2|$; (c) both $|\partial E(C)/\partial \theta_1|$ and $|\partial E(C)/\partial \theta_2|$.

Proposition 3 indicates that the mean travel cost is more sensitive to the lower bound of the degraded capacity (worst condition) under Patterns 1-4, 5b, 5c and 6c. **Numerical finding 2** indicates that no counterexample is found against the fact under other patterns. A numerical example is presented in Figure 8. In Figure 8, θ_1 changes from 0 to 0.5 and θ_2 changes from 0.5 to 1. Figures 8(a) and 8(b) show $|\partial E(C)/\partial \theta_1|$ and $|\partial E(C)/\partial \theta_2|$, respectively in the two-dimensional domain of (θ_1, θ_2), and Figure 8(c) illustrates them in a 3D-coordinate. Given the parameter settings, Patterns 2a, 2b, 2c, 5a, 6a and 6b may occur. $|\partial E(C)/\partial \theta_1| > |\partial E(C)/\partial \theta_2|$ always holds under Patterns 5a, 6a and 6b. Improving the capacity under worst conditions (increasing θ_1) can be more effective in terms of reducing travel cost when compared to increasing the capacity under the "best adverse condition" (increasing θ_2). However, **Remark 4** indicates that it is not necessarily the case for the mean of total queueing time, which is more sensitive to either θ_1 or θ_2.

Proposition 4. *Under Patterns 1-4, 5b, 5c and 6c,* $\partial^2(E(C))/\partial \theta_1^2 > 0$, $\partial^2(E(C))/\partial \theta_2^2 > 0$. *Under Patterns 1-3, 5b, 5c and 6c,* $\partial^2(E(C))/\partial \pi^2 < 0$, *and under Pattern 4,* $\partial^2(E(C))/\partial \pi^2 = 0$.

Numerical finding 3. *Under Patterns 5a, 6a and 6b,* $\partial^2(E(C))/\partial \theta_1^2 > 0$, $\partial^2(E(C))/\partial \theta_2^2 > 0$ and $\partial^2(E(C))/\partial \pi^2 < 0$.

Proposition 4 indicates that with the increase of θ_1 and θ_2, the decreasing rate of mean travel cost becomes smaller under Patterns 1-4, 5b, 5c and 6c. **Numerical finding 3** indicates that no counterexample is found against the fact under other patterns. Numerical examples are presented in Figure 9. This means that the marginal efficiency of improving the degraded capacity diminishes. However, with the decrease of π, the decreasing rate of mean travel cost becomes larger in Patterns 1-3, and 5-6, and in Pattern 4, the mean travel cost decreases linearly.

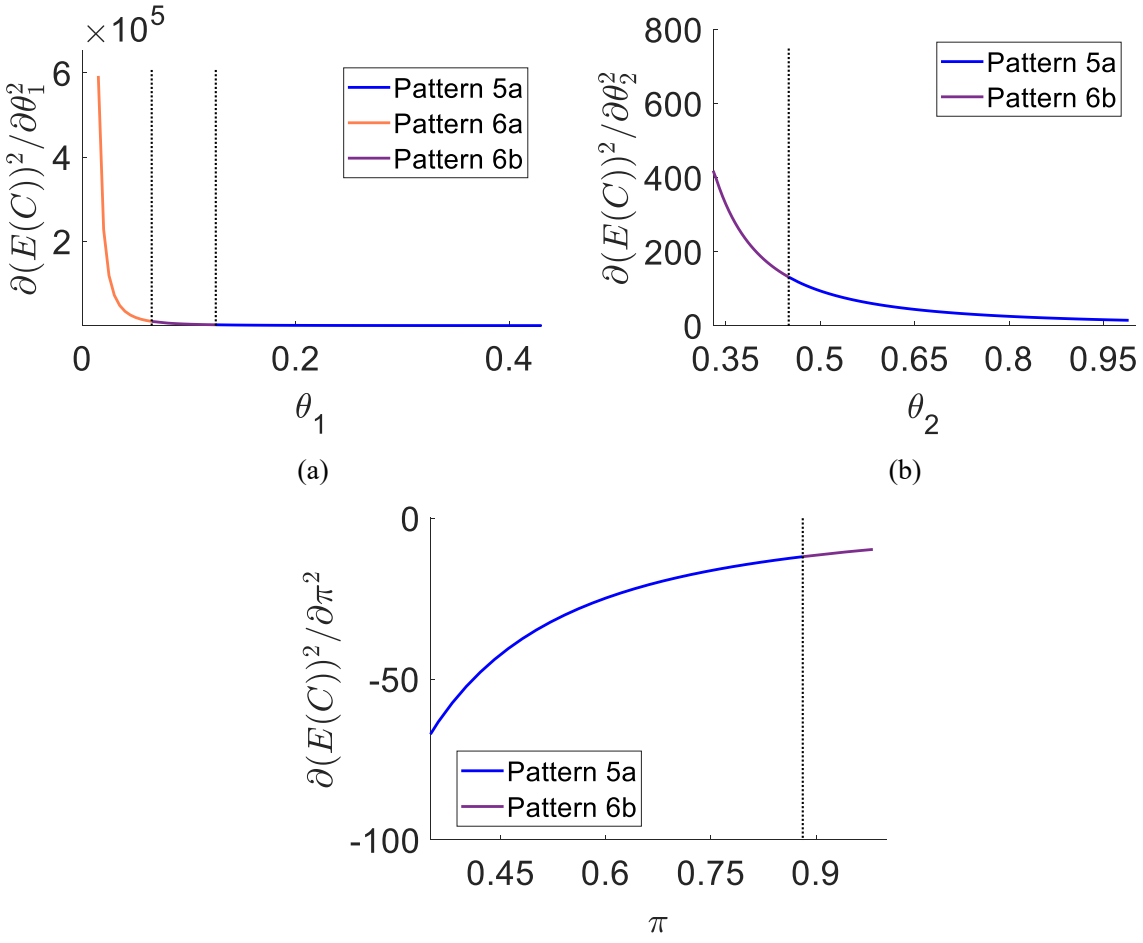

Figure 9. (a) $\partial^2(E(C))/\partial\theta_1^2$ vs. θ_1. $\theta_2 = 0.8$, $\pi = 0.9$. (b) $\partial^2(E(C))/\partial\theta_2^2$ vs. θ_2. $\theta_1 = 0.2$, $\pi = 0.7$. (c) $\partial^2(E(C))/\partial\pi^2$ vs. π. $\theta_1 = 0.2$, $\theta_2 = 0.6$.

4. Numerical Results

In this section, some further numerical examples are provided to facilitate understanding of the commuting patterns under the "mixed" capacity distribution. We show how different parameters may affect the occurrence of different departure/arrival patterns (referred to as "pattern diagram"), the mean travel cost, the congestion level. Moreover, by utilizing the capacity reduction data from the study of Qin and Smith (2001), the comparisons of the results under different capacity distributions have been carried out. Unless otherwise specified, the parameters used in Section 3 are also adopted in this section.

4.1 Impacts of π and θ_1/θ_2 on the occurrence of different patterns

The "pattern diagrams" exhibiting the occurrence regions of different patterns in the plane of $\theta_2 - \pi$ and $\theta_1/\theta_2 - \theta_2$ are shown in Figures 10(a)-(b) and 10(c)-(d), respectively. Note that the "pattern diagrams" depend on the ratios of β/α and γ/α, and Pattern 3a will never arise under the given ratios by Small (1982) according to the boundary conditions summarized in Table 6. Here, β/α=0.269 and γ/α=1.049 are adopted for the purpose of illustrating all the results in Table 6. We have the following

observations.

Firstly, from Figure 10, it is straightforward to confirm that conditions given in Table 6 are mutually exclusive. Secondly, given α, β and γ, π_C is a fixed value as defined in Section 2.2. When the value of θ_1/θ_2 is relatively small, $\pi = \pi_C$ is a redundant boundary condition, which can be seen by comparing Figures 10(a), (b) and (c). In contrast, when θ_1/θ_2 exceeds a critical value denoted as ϑ_C, the pattern diagram exhibits qualitative change at $\pi = \pi_C$, as shown in Figures 10(b) and (c). As given in Table 6, when $\pi < \pi_C$, the diagram will involve seven departure/arrival patterns, i.e., Patterns 4, 5a, 5b, 5c, 6a, 6b, 6c, see Figure 10(d). However, when $\pi > \pi_C$, Patterns 4, 5b, 5c, 6c will not occur. Instead, Patterns 1, 2a, 2b, 2c, 3b, 3c emerge, see Figure 10(e). Finally, when $\theta_1 = \theta_2$, the stochastic capacity follows a binary distribution and six patterns can arise, i.e., Patterns 1, 2c, 3c, 4, 5c, 6c, see Figure 10(c). When $\pi = 1$, the model reduces to the stochastic bottleneck model with continuous distribution of capacity and only Patterns 1, 2, 3 and 6 may occur under the given parameters of α, β and γ, see Figure 10(f).

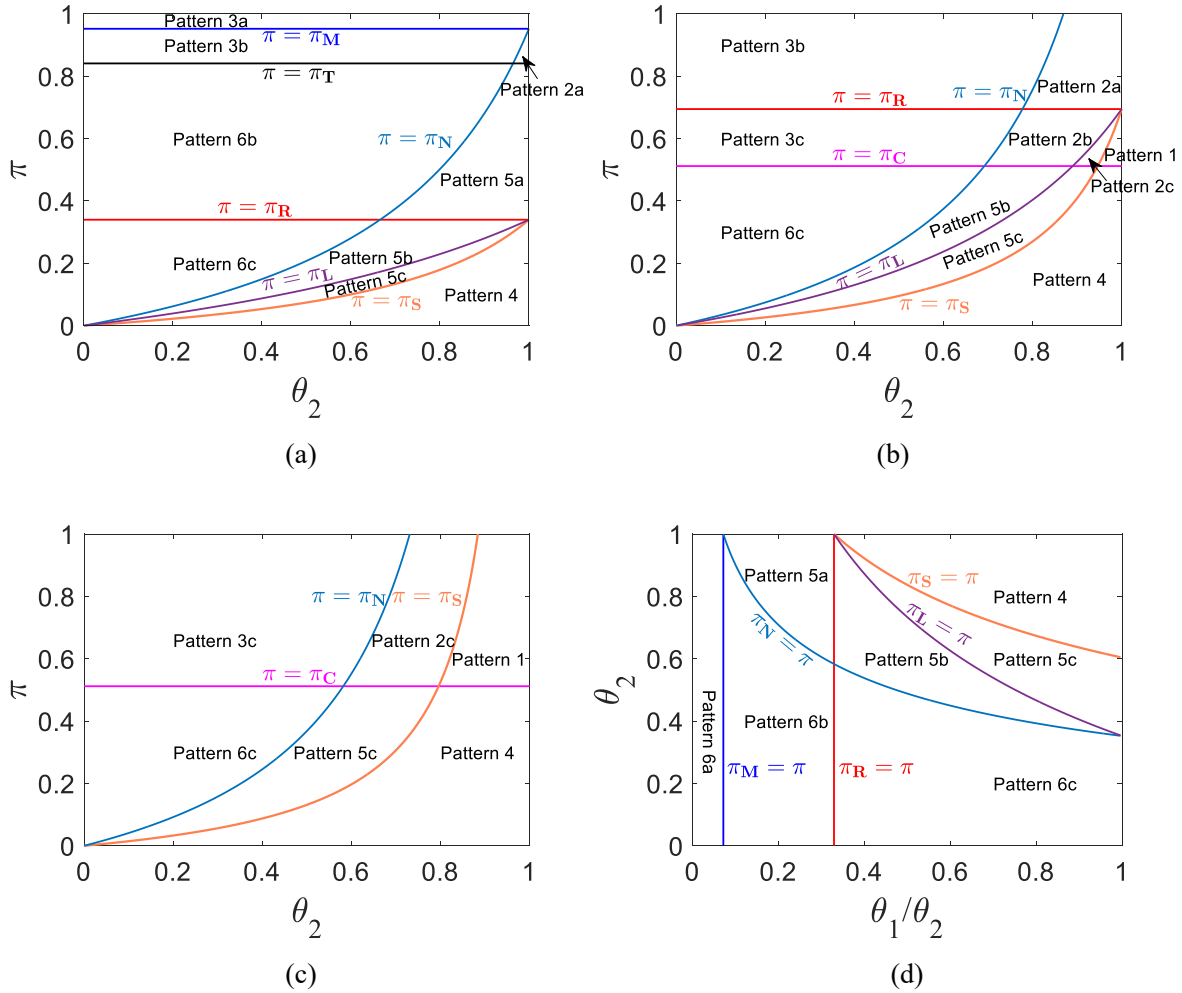

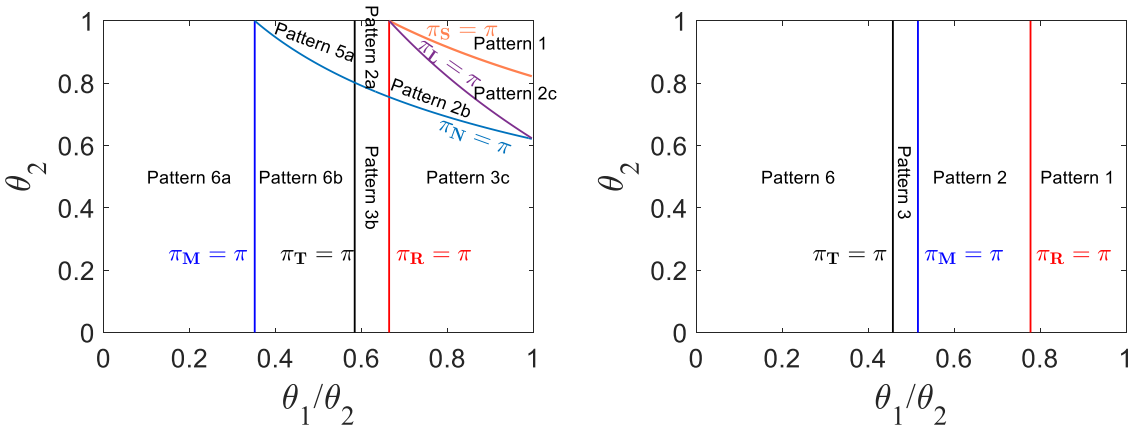

(e) (f)

Figure 10. (a) $\theta_1 = 0.5\theta_2$, (b) $\theta_1 = 0.7\theta_2$, (c) $\theta_1 = \theta_2$, (d) $\pi = 0.2$, (e) $\pi = 0.6$, (f) $\pi = 1$.

4.2 Impacts of m, π, θ_1 and θ_2 on mean travel cost

As mentioned in Section 3, the formulations of mean travel costs in Patterns 1-3 are identical, and those for Patterns 5a, 6a and 6b are identical, and those for Patterns 5b, 5c and 6c are also identical. There are actually 4 types of results for the 14 patterns in total. For simplicity, we do not enumerate all those patterns here. We only illustrate the 4 types of results by examples.

As can be seen from Figure 11, given the mean degraded capacity, the mean travel cost increases with the width of degraded capacity range and the results are in line with Proposition 1 and Numerical finding 1. Therefore, the mean travel cost will be underestimated if the degraded capacity range is ignored.

Figures 12-14 show the variation of mean travel cost and the second derivative of mean travel cost with respect to π, θ_1 and θ_2, respectively. From Figures 12(a) and 12(c), the mean travel cost increases with the increase of π. As shown in Figures 12(b) and 12(d), $\partial^2(E(C))/\partial\pi^2 = 0$ under Pattern 4 and $\partial^2(E(C))/\partial\pi^2 < 0$ under other Patterns. This indicates that with the decrease of π, the decreasing rate is independent of π under Pattern 4 and becomes larger under other patterns. The results are consistent with those in Section 3.

From Figures 13(a), 13(c), 14(a) and 14(c), one can also observe that the mean travel cost decreases with the increase of θ_1 and θ_2 under Patterns 1-6. As can been seen from Figures 13(b), 13(d), 14(b) and 14(d), $\partial^2(E(C))/\partial\theta_1^2 > 0$ and $\partial^2(E(C))/\partial\theta_2^2 > 0$ always hold and the decreasing rate becomes smaller when increasing θ_1 and θ_2 under these patterns, which is in line with the results in Section 3.

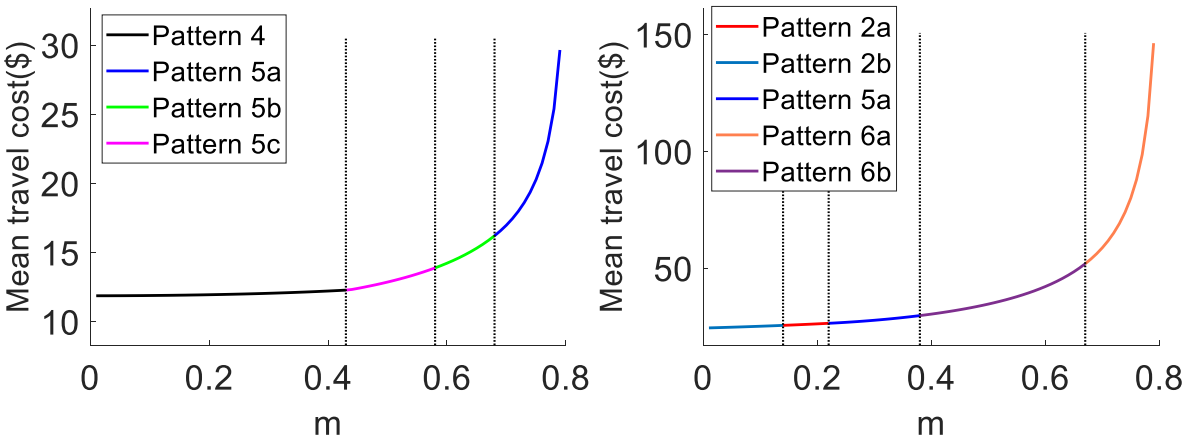

(a) (b)

Figure 11. Impact of m on mean travel cost. (a) $e = 0.4,\ \pi = 0.1$, (b) $e = 0.4,\ \pi = 0.9$.

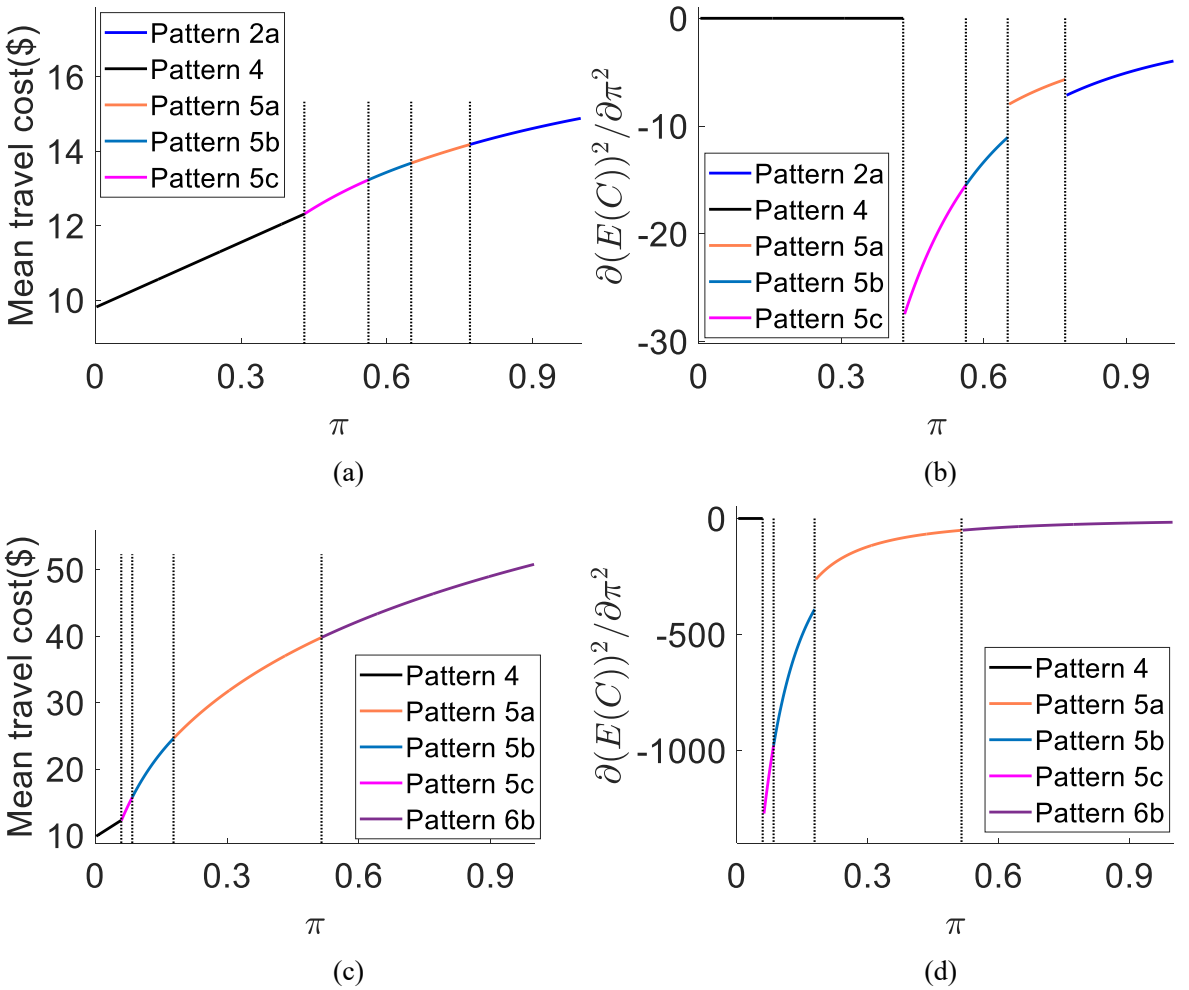

(a) (b)

(c) (d)

Figure 12. Impact of π on mean travel cost. (a)-(b) $\theta_1 = 0.54,\ \theta_2 = 0.9$, (c)-(d) $\theta_1 = 0.1,\ \theta_2 = 0.5$.

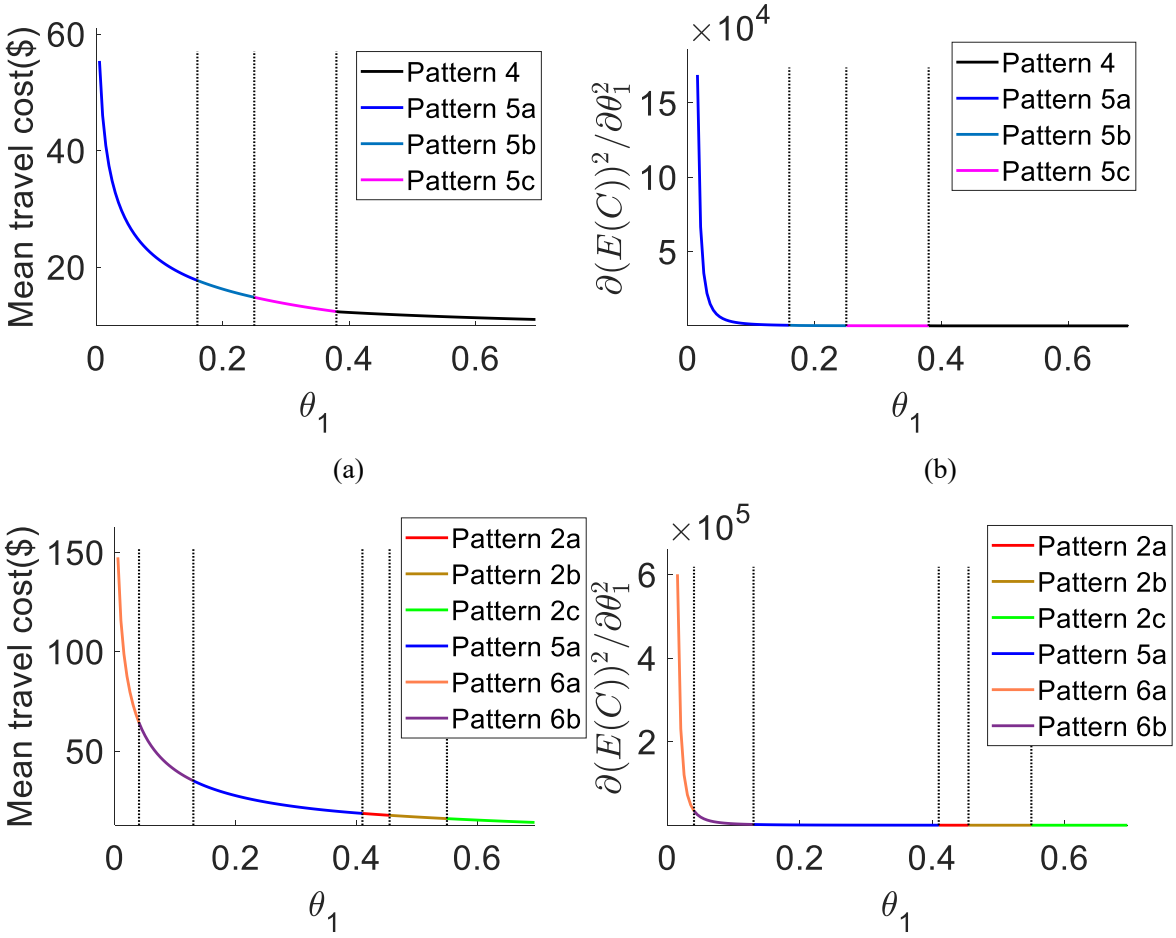

Figure 13. Impact of θ_1 on mean travel cost. (a)-(b) $\theta_2 = 0.7,\ \pi = 0.2$, (c)-(d) $\theta_2 = 0.7,\ \pi = 0.8$.

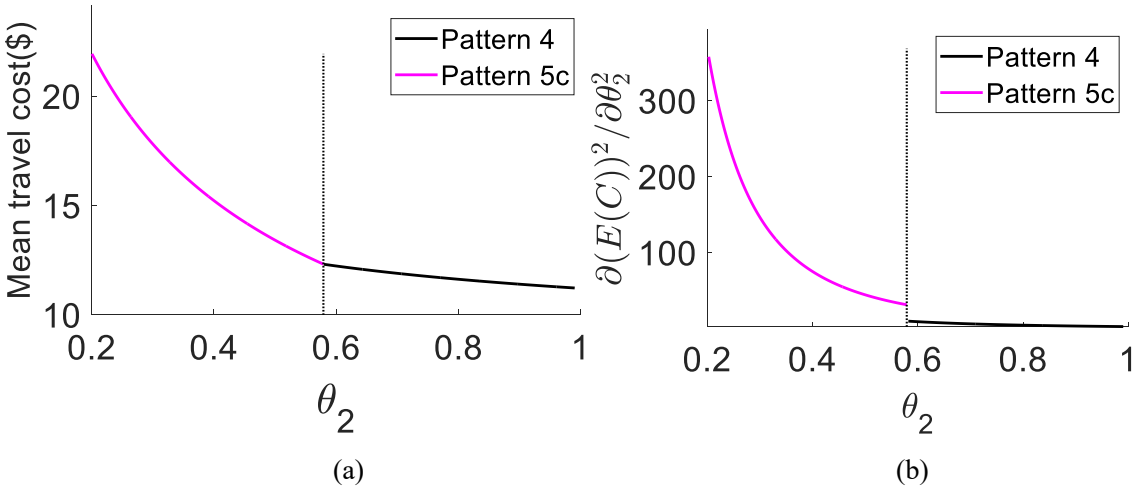

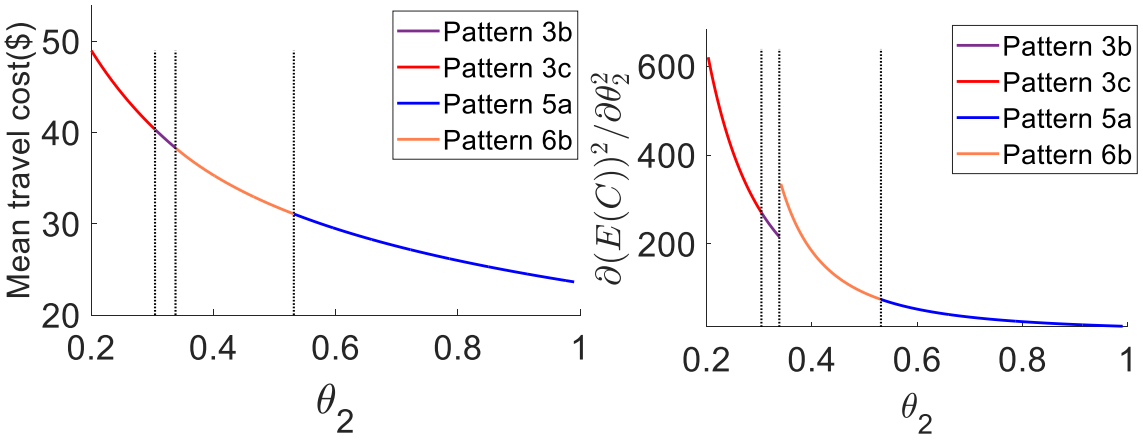

(c) (d)

Figure 14. Impact of θ_2 on mean travel cost. (a)-(b) $\theta_1 = 0.2,\ \pi = 0.1$, (c)-(d) $\theta_1 = 0.2,\ \pi = 0.8$.

4.3 The congestion level

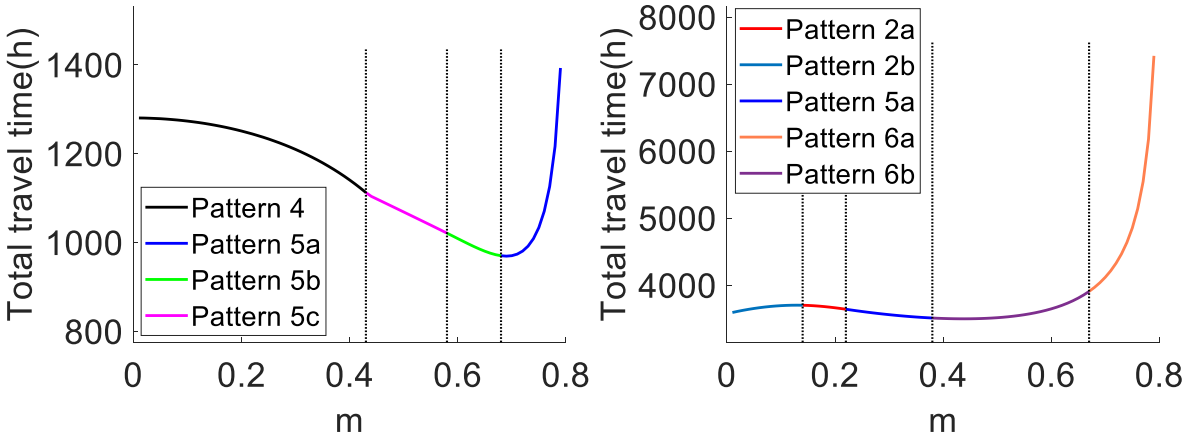

(a) (b)

Figure 15. Impact of m on total travel time. (a) $e = 0.4,\ \pi = 0.1$, (b) $e = 0.4,\ \pi = 0.9$.

The total travel time of system measures the system's congestion level. Figure 15 illustrates how the degraded capacity range affects the mean total travel time under the given mean capacity. As pointed in Section 3, the mean total travel time may be either underestimated or overestimated depending on parameters. Under Pattern 5a, it can be either underestimated when the probability of capacity degradation is relatively small, as shown in Figure 15(a), or overestimated when the probability of capacity degradation is relatively large, as shown in Figure 15(b).

Figures 16-18 illustrate the variations of mean total travel time with respect to π, θ_1 and θ_2, respectively. We have the following observations. Firstly, when the ratio of θ_1/θ_2 is relatively small, the total travel time might increase with the decrease of π, as shown in Figure 16(a). Secondly, as can be seen from Figures 17(a) and 18(a), when $\pi = 0.1$, the total travel time first decreases then increases with respect to θ_1 and θ_2. Furthermore, with a relatively large π, the total travel time decreases with the increase of θ_1 and θ_2, as illustrated in Figures 17(b) and 18(b).

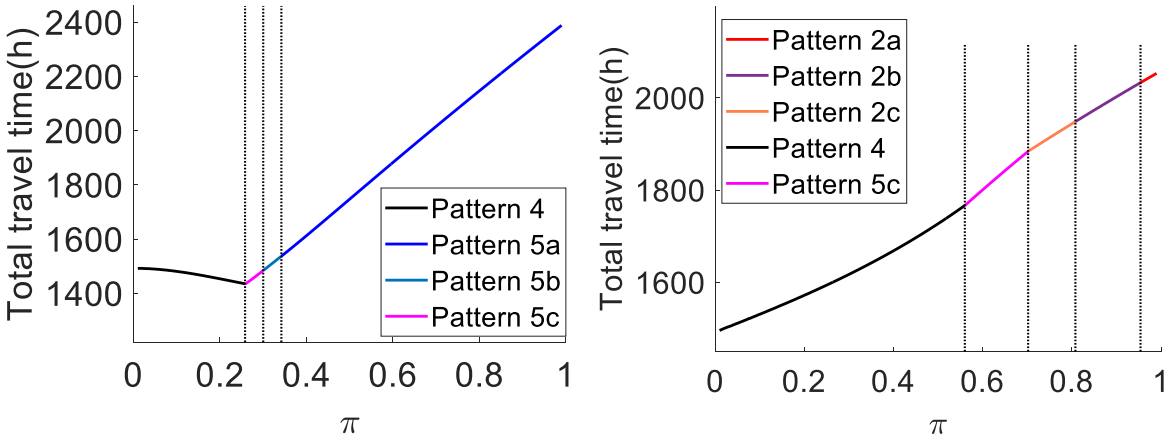

(a) (b)

Figure 16. Impact of π on total travel time. (a) $\theta_1 = 0.36,\ \theta_2 = 0.9$, (b) $\theta_1 = 0.63,\ \theta_2 = 0.9$.

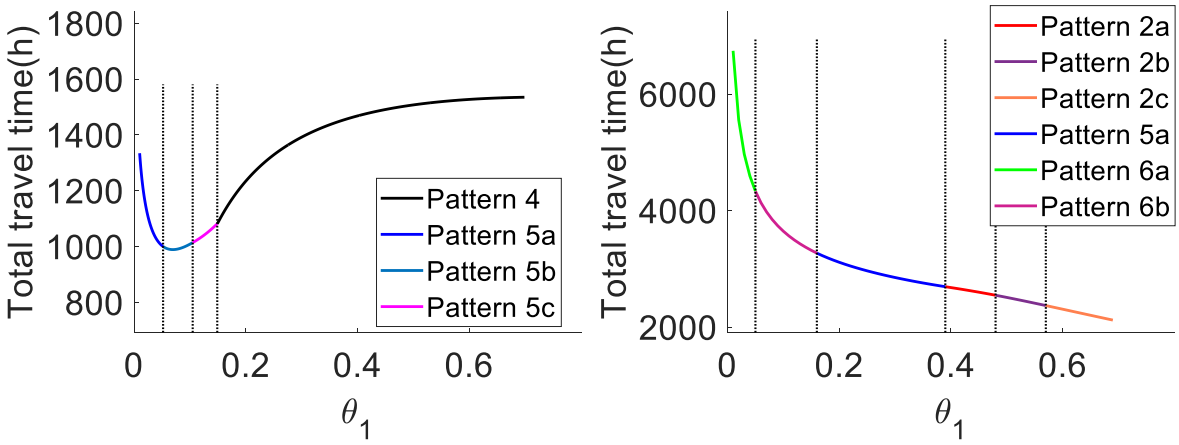

(a) (b)

Figure 17. Impact of θ_1 on total travel time. (a) $\theta_2 = 0.7,\ \pi = 0.1$, (b) $\theta_2 = 0.7,\ \pi = 0.9$.

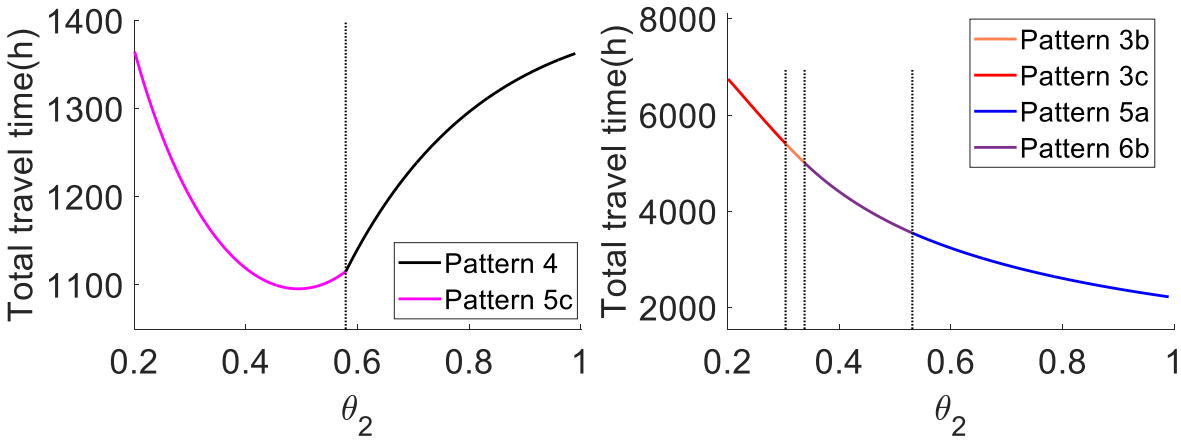

(a) (b)

Figure 18. Impact of θ_2 on the system's total travel time. (a) $\theta_1 = 0.2,\ \pi = 0.1$, (b) $\theta_1 = 0.2,\ \pi = 0.8$.

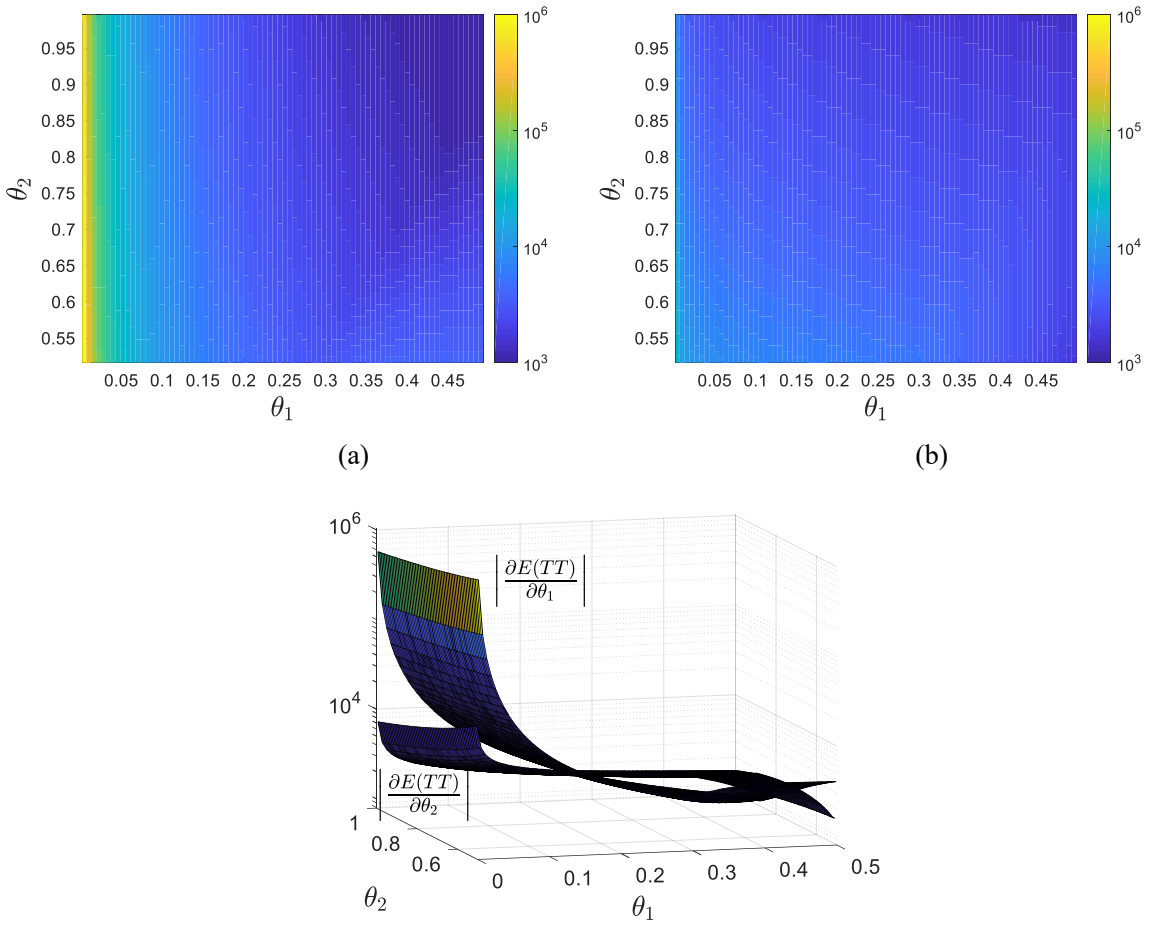

Figure 19. The comparison of impacts of θ_1 and θ_2 on total travel time. $\pi = 0.9$. (a) $|\partial E(TT)/\partial \theta_1|$; (b) $|\partial E(TT)/\partial \theta_2|$; (c) both $|\partial E(TT)/\partial \theta_1|$ and $|\partial E(TT)/\partial \theta_2|$.

Figure 19 compares the impacts of θ_1 and θ_2 on the total travel time, where θ_1 changes from 0 to 0.5 and θ_2 changes from 0.5 to 1. Figures 19(a) and 19(b) show $|\partial E(TT)/\partial \theta_1|$ and $|\partial E(TT)/\partial \theta_2|$ in the two-dimensional plane of $\theta_1 - \theta_2$ and Figure 19(c) further illustrates them in a 3D-coordinate. Under the current parameter settings, Patterns 2a, 2b, 2c, 5a, 6a and 6b may occur, and the total travel time always decreases with both θ_1 and θ_2. However, the results show that improving θ_1 is not necessarily more effective than θ_2 on alleviating the total congestion level.

The standard deviation of the system's travel time (which fluctuates from day to day due to the capacity uncertainty) can be used to aggregately measure the level of uncertainty faced by commuters. In the system with a higher standard deviation of travel time, commuters are less likely to arrive at the destination at their expected arrival times. Figures 20-22 show the changes of the standard deviation of system's travel time with respect to π, θ_1 and θ_2, respectively.

From Figure 20, one can observe that with the increase of π, the standard deviation of total travel time first increases and then decreases. When π is relatively small, increasing π means increasing capacity variability and thus results in a larger variation in travel time. When π is relatively large, capacity reduction becomes "more certain". Therefore, capacity variability may indeed reduce, which results in less variation in the travel time.

We further observe from Figure 21 that improving the capacity under the worst condition can always

reduce the travel time variation of the system, while it may not apply for increasing θ_2 as shown in Figure 22. Moreover, we observe that under a relatively large π, the capacity reduction is quite likely to occur, the system variability mainly comes from the capacity variation within the degraded capacity range. In such a case, increasing θ_2 yields a larger variation of capacity, which can result in more travel time variations, as can be seen from Figure 22(b).

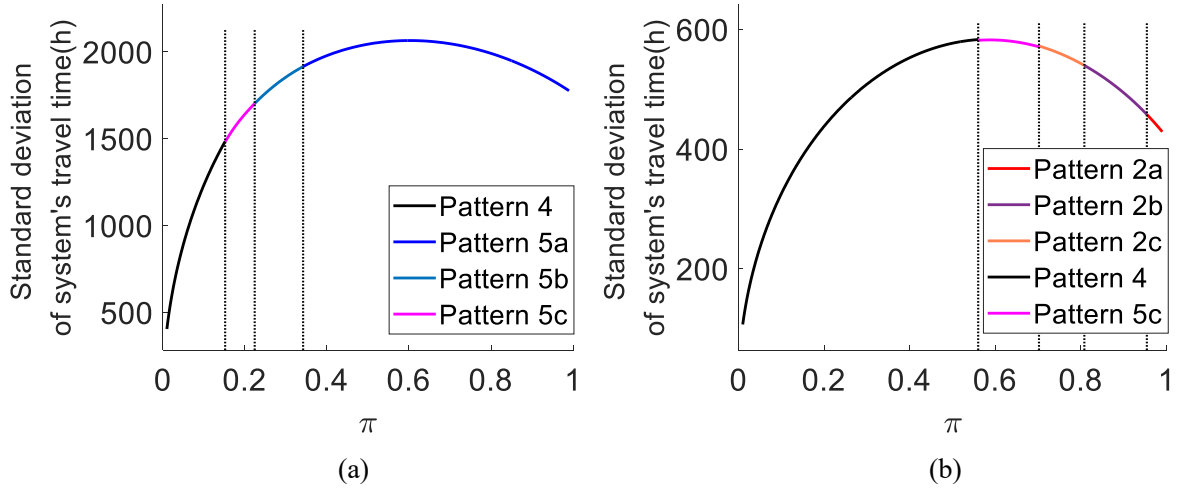

(a) (b)

Figure 20. Impact of π on standard deviation of system's travel time. (a) $\theta_1 = 0.28,\ \theta_2 = 0.7$, (b) $\theta_1 = 0.63,\ \theta_2 = 0.9$.

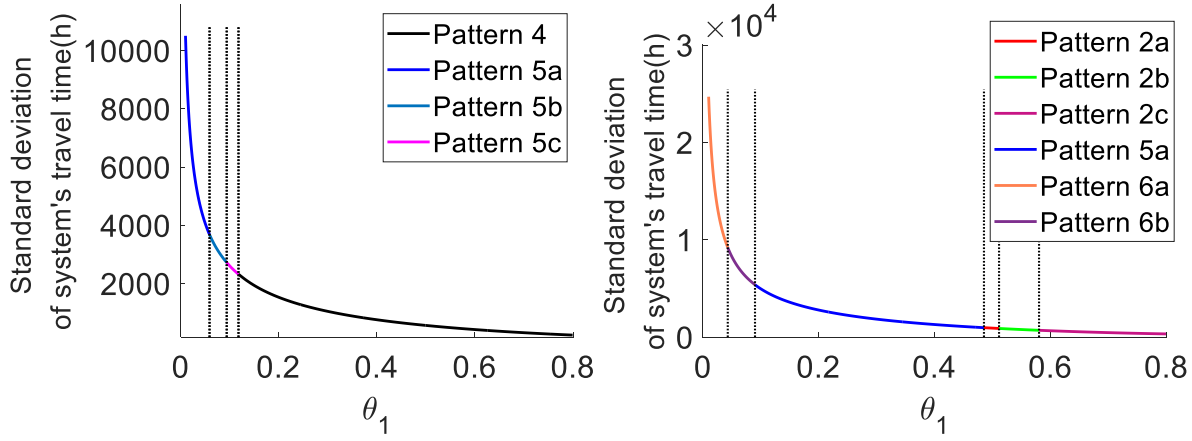

(a) (b)

Figure 21. Impact of θ_1 on standard deviation of system's travel time. (a) $\theta_2 = 0.8,\ \pi = 0.1$, (b) $\theta_2 = 0.8,\ \pi = 0.75$.

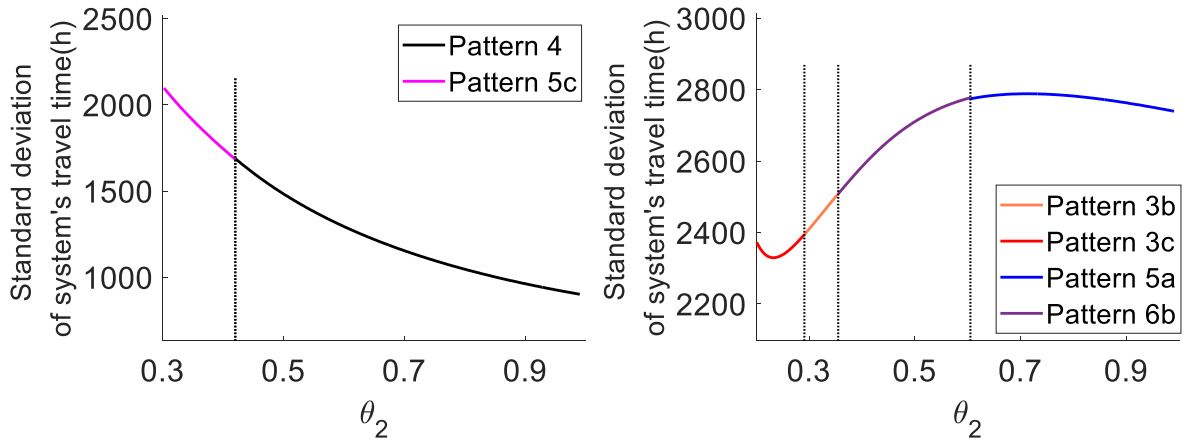

(a) (b)

Figure 22. Impact of θ_2 on standard deviation of system's travel time. (a) $\theta_1 = 0.3$, $\pi = 0.1$, (b) $\theta_1 = 0.2$, $\pi = 0.9$.

4.4 Comparison: different capacity distributions

This subsection further numerically examines and compares the impacts of different capacity distributions on the commuting. The accidents capacity reductions due to one lane and two lanes (out of three lanes) being blocked were fitted with the Beta distribution in the empirical study by Qin and Smith (2001). For simplicity, here we only consider the case when one lane (out of three lanes) is blocked. We adopt the observed accident capacity reductions given in the histogram in Figure 4.9 of Qin and Smith (2001). Based on the capacity data, we can obtain the resulting equilibrium departure/arrival patterns. Specifically, we first need to guess the initial departure time, and compute the equilibrium departure rate. Then, we will check whether the last traveler incurs the same expected travel cost as the first traveler. If not, another value of the initial departure time is chosen. The process is repeated until the equilibrium is achieved. This is similar to that proposed in Liu and Geroliminis (2016).

To be comparable, the probability of incidents, the designed capacity and the mean capacity under different distributions are assumed to be the same (we consider the observed accident capacity in Qin and Smith (2001), the binary capacity distribution and the proposed "mixed" distribution in the current study). Since the probability of incidents on the road is not given in Qin and Smith (2001), the comparisons under the different probabilities of incidents will be illustrated.

From the data observed in one lane out of three lanes blocked (Qin and Smith, 2001), the mean percentage of accident capacity reduction is 62.65%. Therefore, for the binary distribution, the degraded ratio of capacity is 0.3735. The maximum percentage of accident capacity reduction observed in the empirical study by Qin and Smith (2001) is 90.69% (9.31% capacity remains). For the "mixed" capacity distribution assumed in the current study, we thus adopt θ_1 =0.0931. Then, we have θ_2 =0.6539 to ensure the same mean capacity as that in Qin and Smith (2001). Given these parameter values, the equilibrium patterns can be identified as Patterns 5b, 5a or 6b when π changes from 0 to 1, which indicates that these three patterns are more likely to occur.

In Figure 23, "Line O", "Line 1" and "Line 2" illustrate the cumulative departure curves obtained from the observed data, binary distribution and "mixed" distribution assumed in this study, respectively. We have the following observations. Firstly, given the parameters in Figure 23, Pattern 5a occurs. Commuters depart no later than the work start time during the morning peak. Secondly, compared with that

obtained from the observed capacity data, the morning peak begins earlier when the degraded capacity follows the uniform distribution, and it begins later when the degraded capacity is considered as a value. This indicates that "mixed" distribution of capacity studied in the current paper overestimates the departure duration (this might be addressed by relax the assumption of uniform distribution for the degraded capacity), while binary distribution of capacity underestimates the departure duration. Furthermore, "mixed" distribution of capacity assumed in the current study can give a better interpretation of the equilibrium patterns than the binary-distributed capacity. As can be seen from Figure 23(a), when the adverse condition is less likely to occur, i.e., π is relatively small, the departure pattern after 7.8h under the "mixed" capacity distribution is almost identical to that obtained from the observed data. Nevertheless, the uniform distribution of degraded capacity always overestimates the cumulative departure of each departure time. Conversely, when the degraded capacity range is considered as a constant value, the cumulative number of commuters at each departure time is always underestimated under a relatively small probability of incidents see Figure 23(a), while it might be either underestimated or overestimated (depending on the departure times) under a relatively large probability of incidents, see Figure 23(b).

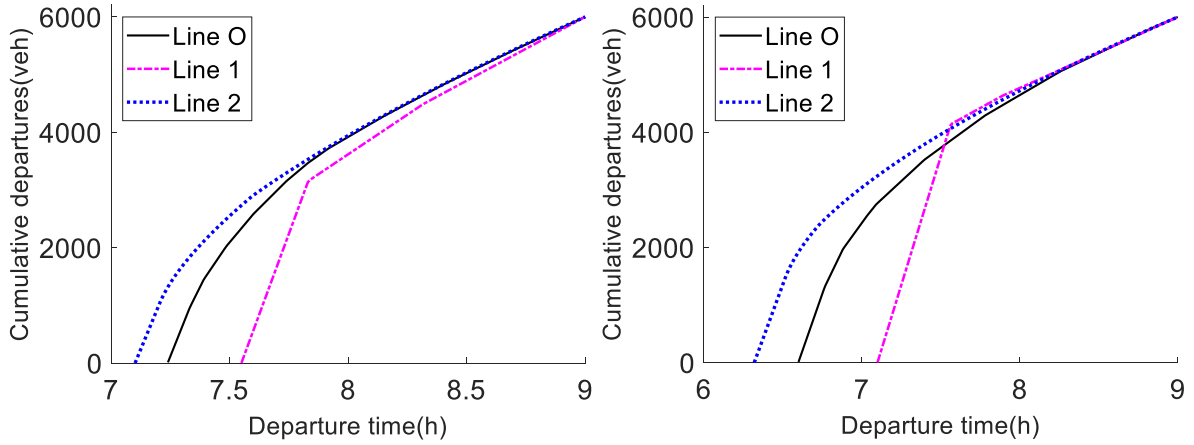

Figure 23. Equilibrium patterns under different capacity distributions. (a) $\pi = 0.2$, (b) $\pi = 0.4$.

Denote EC_j, AQC_j and ASC_j as expected travel cost, average queuing cost and average schedule delay cost calculated from the capacity distribution j, respectively. The subscript j=O, 1 and 2 denote the observed capacity data, the binary capacity distribution and the "mixed" capacity distribution assumed in the current study, respectively. Define $w_i^{EC} = 1 - |EC_O - EC_i|/EC_O$, $w_i^{AQC} = 1 - |AQC_O - AQC_i|/AQC_O$, and $w_i^{ASC} = 1 - |ASC_O - ASC_i|/ASC_O$ as the accuracy of capacity distribution i when estimating expected travel cost, average queuing cost and average schedule delay cost, respectively, and i=1 and 2. The results are illustrated in Figure 24. "Line O", "Line 1" and "Line 2" represent those under the observed data, binary capacity distribution and "mixed" capacity distribution, respectively. We have the following observations.

Firstly, as shown in Figure 24(a), the mean travel cost is overestimated by the uniform distribution of degraded capacity, and it is underestimated when the degraded capacity range is considered as a value. The results are in line with Proposition 1. From Figures 24(a) and 24(b), with the increase of the probability of incidents, the errors of *EC* estimated by the two distributions increase. However, the accuracy of "mixed" capacity distribution assumed in the current study is always greater than 80%. Secondly, the "mixed" distribution also has the better performance to estimate the average queuing cost and the average schedule delay cost, with the accuracy above 90% and 80%, respectively. By contrast, the performance is worse

when the degraded capacity is considered as a constant value. Under the cases, the average queuing cost is overestimated, and the average schedule delay cost is underestimated, compared with those under the other two capacity distributions. Finally, the uniform distribution of degraded capacity always overestimates the mean travel cost and the average schedule delay cost, and may either underestimate or overestimate the average queuing cost depending on the probability of incidents.

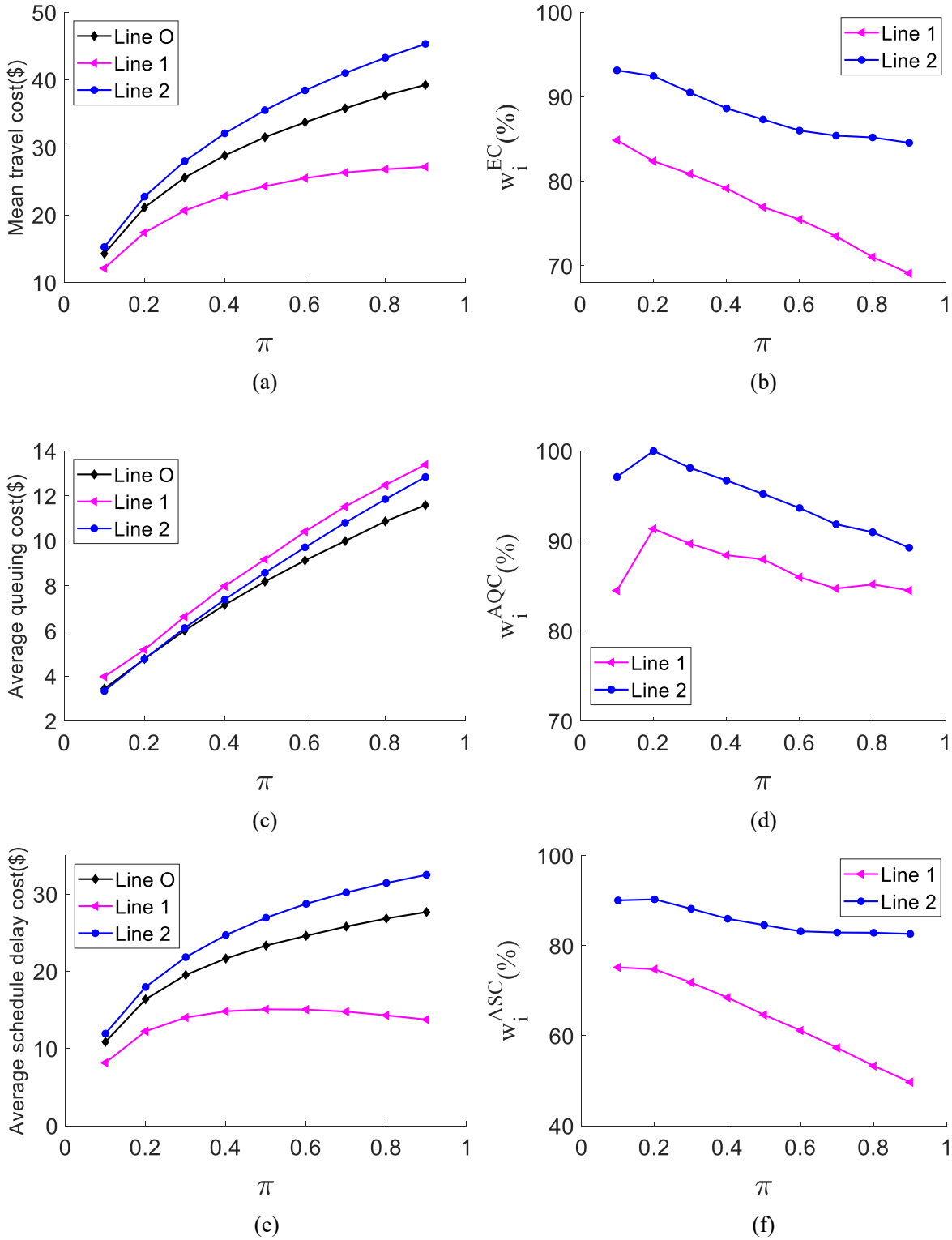

Figure 24. (a) *EC*, (b) w_i^{EC}, (c) AQC, (d) w_i^{AQC}, (e) ASC, (f) w_i^{ASC}.

5. Conclusion

This paper examines the morning commute problem with stochastic highway bottleneck capacity, where the capacity is constant within a day but changes stochastically from day-to-day. In order to account for the variability of capacity caused by incidents and other factors, this paper extends existing studies by considering a more general capacity distribution. In particular, the capacity follows a "mixed" distribution, which is at the designed value under good external conditions, while it degrades into a smaller value falling within an interval under adverse conditions with a certain probability. Commuters are assumed to make the departure time choices following Wardrop's first principle in terms of the mean travel cost. Six possible equilibrium departure/arrival patterns and 14 sub-patterns are identified. Different possible equilibrium departure/arrival patterns are analyzed theoretically and the boundary conditions for their occurrence are also obtained analytically. This study indicates that the capacity degradation probability can substantially affect equilibrium departure patterns and travel cost, and further enhances our understanding on the morning commute problem given the "mixed" distribution of highway bottleneck capacity.

The impacts of capacity degradation probability and the ratios of degraded capacity on the mean travel cost are examined both analytically and numerically, and those on the system's travel time and standard deviation of system's travel time are further investigated numerically to measure the congestion level and the variability of the system. The results show that the mean travel cost decreases with the increase of degraded capacity and with the decrease of capacity degradation probability under all possible equilibrium departure/arrival patterns. However, improving the degradation of capacity when the adverse condition rarely happens or reducing the capacity degradation probability when the ratio of θ_1/θ_2 is relatively small might exacerbate system's congestion. Although improving the capacity under the "worst condition" (increasing θ_1) can be more effective to reduce the mean travel cost than improving the capacity under the "best adverse condition" (increasing θ_2), it is not always the case for reducing the total travel time. Furthermore, in terms of reducing the mean travel cost, the marginal efficiency of increasing the degraded ratios of capacity diminishes with the improvement of capacity degradation, while that of reducing the capacity degradation probability increases or does not change with the improvement of frequency of adverse condition. Finally, numerical results show that the travel time variation of the system can always be reduced by improving the capacity under "worst condition", while increasing the upper bound of capacity or reducing the capacity degradation probability might not always be the case.

In order to lower the mean travel cost of commuters, reducing the probability of adverse condition tends to be more effective. When the measures of improving the degraded capacity are adopted, whether the system's congestion becomes worse or not should be carefully monitored, especially when the incidents are less likely to occur.

In order to further quantify the differences between when the degraded capacity range is considered as a constant value and when the degraded capacity follows uniform distribution defined in the current study, the impact of width of the degraded capacity range under the given mean capacity is analyzed analytically. The results indicate that given the mean capacity, the mean travel cost would be underestimated if the capacity degradation range is considered as a fixed value. Based on the empirical study by Qin and Smith (2001), comparisons of the results under the observed capacity data, the "mixed" distribution assumed in this study and binary distribution are illustrated numerically. It is found that the identified Patterns 5a, 5b and 6b are more likely to occur in practice and commuters depart no later than the work start time when facing uncertainty. The "mixed" distribution assumed in this study always has a better representation in evaluating the departure pattern, mean travel cost, average queuing cost and average

schedule delay cost than that when the degraded capacity range is considered as a constant. Nevertheless, the mean travel cost is always overestimated if the degraded capacity is assumed to follow the uniform distribution under the given mean capacity.

This study can be further extended in several aspects. Firstly, this study focuses on risk-neutral commuters. Further incorporating and exploring commuters' diverse attitudes towards risk can further help to understand the choice behavior of commuters when they face uncertainty. Secondly, only no-toll equilibrium has been investigated in this study. Since queuing delay in bottleneck model is a deadweight loss, the tolling scheme to reduce congestion and achieve the social optimum can be analyzed, where the capacity stochasticity should be considered. Additionally, commuters may have different values of time and risk attitudes in reality. It is of our interest to further study commuter heterogeneity in both no-toll scenario and step toll or fine toll scenario (Arnott et al., 1994; Van den Berg and Verhoef, 2011; Van den Berg, 2014). This study may also be extended to examine or incorporate morning-evening integrated commute (Zhang et al., 2005; Zhang et al., 2019), price-sensitive demand (Arnott et al., 1993; Yang and Huang, 1997; Jiang et al., 2021), the ridesharing mode (Ma and Zhang, 2017; Liu and Li, 2017; Wei et al., 2022), demand uncertainty (Sun et al., 2011) and parking management (Qian et al., 2012; Yang et al., 2013).

Acknowledgement. We would like to thank the useful comments from the reviewers, which helped improve this paper substantially. This work is supported by the National Natural Science Foundation of China under Grant No. 72288101, No. 71931002.

Online Appendix

Appendix can be found in the online Supplemental file.

Reference

Agarwal, M., Maze, T.H., Souleyrette, R., 2005. Impacts of weather on urban freeway traffic flow characteristics and facility capacity. In: Proceedings of the 2005 Mid-Continent Transp. Res. Sym., Ames, Iowa, 18-19 Aug. 2005.

Arnott, R., de Palma, A., Lindsey, R., 1990. Economics of a bottleneck. J. Urban Econ. 27 (1), 111-130.

Arnott, R., de Palma, A., Lindsey, R., 1993. A structural model of peak-period congestion: a traffic bottleneck with elastic demand. Am. Econ. Rev. 83 (1), 161-179.

Arnott, R., de Palma, A., Lindsey, R., 1994. The welfare effects of congestion tolls with heterogeneous commuters. J. Transp. Econ. Policy 28 (2), 139-161.

Arnott, R., de Palma, A., Lindsey, R., 1999. Information and time-of-usage decisions in the bottleneck model with stochastic capacity and demand. Eur. Econ. Rev. 43 (3), 525-548.

Chen, A., Zhou, Z., 2010. The α-reliable mean-excess traffic equilibrium model with stochastic travel times. Transp. Res. Part B 44 (4), 493-513.

Chen, A., Zhou, Z., Lam, W.H.K., 2011. Modeling stochastic perception error in the mean-excess traffic equilibrium model. Transp. Res. Part B 45 (10), 1619-1640.

Fosgerau, M., 2008. Congestion costs in bottleneck with stochastic capacity and demand. Munich Pers. RePEc Arch. Pap. Univ. Libr of Munich, German.

Fosgerau, M., 2010. On the relation between the mean and variance of delay in dynamic queues with random capacity and demand. J. Econ. Dynam. Control 34 (4), 598-603.

Jiang, G., Lo, H.K., 2016. The impact of cost variability in a bottleneck model with heterogeneous random delay. Smart Transportation: The 21st International Conference of Hong Kong Society for Transportation Studies (HKSTS), Hong Kong.

Jiang, G., Lo, H.K., Tang, Q.R., Liang, Z., Wang, S.L., 2021. The impact of road pricing on travel time variability under elastic demand, Transportmetrica B: Transport Dynamics, 9(1), 595-621.

Jiang, G., Wang, S.L., Lo, H.K., Liang, Z., 2022. Modeling cost variability in a bottleneck model with degradable capacity, Transportmetrica B: Transport Dynamics, 10(1), 84-110.

Li, H., Bliemer, M.C.J., Bovy, P.H.L., 2008. Departure time distribution in the stochastic bottleneck model. Internat. J. ITS Res. 6 (2), 79-86.

Li, H., Tu, H., Zhang, X., 2017. Travel time variations over time and routes: endogenous congestion with degradable capacities. Transport. B 5 (s1), 56-77.

Li, Z., Huang, H.J., Yang, H., 2020. Fifty years of the bottleneck model: A bibliometric review and future research directions. Transp. Res. Part B 139, 311-342.

Lindsey, R., 1994. Optimal departure scheduling in the morning rush hour when capacity is uncertain. Presented at the 41st North Amer. Meeting of the Regional Sci. Assoc., Niagara Falls, Ontario.

Lindsey, R., Daniel, T., Gisches, E., Rapoport, A., 2014. Pre-trip information and route-choice decisions with stochastic travel conditions: Theory. Transp. Res. Part B 67, 187-207.

Liu, Q.M., Jiang, R., Liu, R.H., Zhao, H., Gao, Z.Y., 2020. Travel cost budget based user equilibrium in a bottleneck model with stochastic capacity. Transp. Res. Part B 139, 1-37.

Liu, W., Geroliminis, N., 2016. Modeling the morning commute for urban networks with cruising-for-parking: An MFD approach. Transp. Res. Part B 93, 470-494.

Liu, Y., Li, Y.Y., 2017. Pricing scheme design of ridesharing program in morning commute problem. Transp. Res. Part C 79, 156-177.

Lo, H.K., Luo, X.W., Siu, B.W.Y., 2006. Degradable transport network: travel time budget of travelers with heterogeneous risk aversion. Transp. Res. Part B 40 (9), 792-06.

Lo, H.K., Tung, Y.K., 2003. Network with degradable links: Capacity analysis and design. Transp. Res. Part B 37 (4), 345-363.

Long, J., Yang, H., Szeto, W.Y., 2022. Departure Time Choice Equilibrium and Tolling Strategies for a Bottleneck with Stochastic Capacity. Transp. Sci. 56(1), 79-102.

Ma, M., Liu, W., Li, X., Zhang, F., Jian, S., Dixit, V., 2021. Quantifying service-reliability-based day-to-day evolution of travel choices in public transit systems with smart transit card data. Transportmetrica B: Transport Dynamics, 9(1), 519-551.

Ma, R., Zhang, H.M., 2017. The morning commute problem with ridesharing and dynamic parking charges. Transport. Res. Part B 106, 345-374.

Nie, Y., 2011. Multi-class percentile user equilibrium with flow-dependent stochasticity. Transp. Res. Part B 45 (10), 1641-1659.

Ozbay, K., Yanmaz-Tuzel, O., 2008. Valuation of travel time and departure time choice in the presence of time-of-day pricing. Transp. Res. Part A 42, 577-590.

Peer, S., Koster, P., Verhoef, E., Rouwendal, J., 2010. Traffic incidents and the bottleneck model. Working paper, Department of Spatial Economics, VU University, Amsterdam, the Netherlands.

Qian, Z., Xiao, F., Zhang, H.M., 2012. Managing morning commute traffic with parking. Transp. Res. Part B 46 (7), 894-916.

Qin, L., Smith., B.L., 2001. Characterization of accident capacity reduction. Report UVACTS-15-0-48. Center for Transportation Studies, University of Virginia, Charlottesville.

Siu, B.W.Y., Lo, H.K., 2009. Equilibrium trip scheduling in congested traffic under uncertainty. Lam W.H.K., Wong, S.C., Lo, H.K., eds. Transportation and Traffic Theory 2009: Golden Jubilee. Hong Kong Springer, US, pp. 19-38.

Small, K. A., 1982. The scheduling of consumer activities: work trips. Am. Econ. Rev., 72(3), 467-479.

Smith, B.L., Byrne, K.G., Copperman, R.B., Hennessy, S.M., Goodall, N.J., 2004. An investigation into the impact of rainfall on freeway traffic flow. In: 85th Annual Meeting of the Transp. Res. Board, Washington DC.

Sun, H., Gao, Z.Y., Long, J.C., 2011. The robust model of continuous transportation network design problem with demand uncertainty. J. Transpn. Sys. Eng. & IT. 11 (2), 70-76.

Van den Berg, V.A.C., 2014. Coarse tolling with heterogeneous preferences. Transp. Res. Part B 64, 1-23.

Van den Berg, V.A.C., Verhoef, E.T., 2011. Congestion tolling in the bottleneck model with heterogeneous values of time. Transp. Res. Part B 45 (1), 60-78.

Vickrey, W.S., 1969. Congestion theory and transport investment. Am. Econ. Rev. (Papers and Proceedings) 59 (2), 251-261.

Watling, D., 2006. User equilibrium traffic network assignment with stochastic travel times and late arrival penalty. Eur. J. Oper. Res. 175 (3), 1539-1556.

Wei, B., Zhang, X., Liu, W., Saberi, M., Waller, S.T., 2022. Capacity allocation and tolling-rewarding schemes for the morning commute with carpooling. Transp. Res. Part C 142, 103789.

Xiao, L.L., Huang, H.J., Liu, R., 2015. Congestion behavior and tolls in a bottleneck model with stochastic capacity. Transp. Sci. 49 (1), 46-65.

Xiao, L.L., Huang, H.J., Tian, L.J., 2014b. Stochastic bottleneck model with heterogeneous travelers. J. Transpn. Sys. Eng. & IT. 14 (4), 93-98.

Xiao, L.L., Liu, R., Huang, H.J., 2014a. Stochastic bottleneck capacity, merging traffic and morning commute. Transp. Res. Part E 64, 48-70.

Yang, H., Huang, H., 1997. Analysis of the time-varying pricing of a bottleneck with elastic demand using optimal control theory. Transp. Res. Part B 31 (6), 425-440.

Yang, H., Liu, W., Wang, X., Zhang, X., 2013. On the morning commute problem with bottleneck congestion and parking space constraints. Transp. Res. Part B 58, 106-118.

Yin, Y., Lam, W.H.K., Ieda, H., 2004. New technology and the modeling of risk-taking behavior in congested road networks. Transp. Res. Part C 12, 171-192.

Yu, Y., Han, X., Jia, B., Jiang, R., Gao, Z.Y., Zhang, H.M., 2021. Is providing inaccurate pre-trip information better than providing no information in the morning commute under stochastic bottleneck capacity?. Transp. Res. Part C 126, 103085.

Zhang, X.N., Yang, H., Huang, H.J., Zhang, H.M., 2005. Integrated scheduling of daily work activities and morning-evening commutes with bottleneck congestion. Transp. Res. Part A 39 (1), 41-60.

Zhang, X., Liu, W., Waller, S.T., Yin, Y., 2019. Modelling and managing the integrated morning-evening commuting and parking patterns under the fully autonomous vehicle environment. Transp. Res. Part B 218, 380-407.

Zhu, Z., Li, X., Liu, W., Yang, H., 2019. Day-to-day evolution of departure time choice in stochastic capacity bottleneck models with bounded rationality and various information perceptions. Transp. Res. Part E 131, 168-192.